

MJO Simulations/Hindcasts with NICAM

T. Nasuno, M. Satoh, K. Oouchi, H. Taniguchi, H. Tomita, S. Iga, A. T. Noda, Y. Yamada, C. Kodama, H. Miura, W. Yanase, H. Yamada, H. Fudeyasu, and JAMSTEC ISV observation team

Research Institute for Global Change, JAMSTEC
Atmosphere and Ocean Research Institute, Univ. of Tokyo
Yokohama National University

Monsoon Intraseasonal Variability Modelling Workshop

June 15-17, 2009

APEC Climate Center, Busan, Korea

[Group web page is http://nicam.jp](http://nicam.jp)



Outlines

- Overview of NICAM

Nonhydrostatic ICosahedral Atmospheric Model for Global Cloud-Resolving Simulations

- Monsoon and ISV simulations with NICAM

Seasonal simulation, sensitivity experiments (SST, physics)

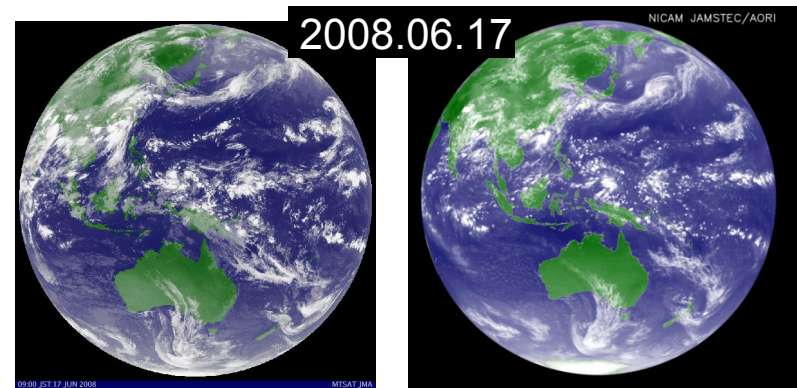
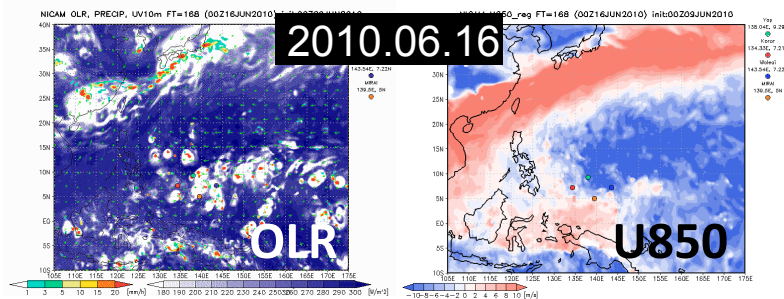
–2004 boreal summer series (Oouchi et al. 2009a,b; Noda et al. 2010) → Oouchi

Collaboration with field observation projects **MISMO** (Poster 6/15)

–2006 boreal winter series (Miura et al. 2007, 2009) → Miyakawa (Poster 6/16)

–2008 boreal summer series (Taniguchi et al. 2011) → **PALAU2008, YOTC** w !)

PALAU2010 (15may-20jun) → Oouchi (Poster)



- Summary and Future plans

NICAM

- Nonhydrostatic Icosahedral Atmospheric Model

Development since 2000

Tomita and Satoh(2005, *Fluid Dyn. Res.*)

Satoh et al.(2008, *J. Comp. Phys.*)

First global $dx=3.5\text{km}$ run in 2004

Tomita et al.(2005, *Geophys. Res. Lett.*)

- Icosahedral grid

Spring dynamics smoothing

Second order accuracy

Tomita et al.(2001, *J. Comp. Phys.*), Tomita et al.(2002, *J. Comp. Phys.*)

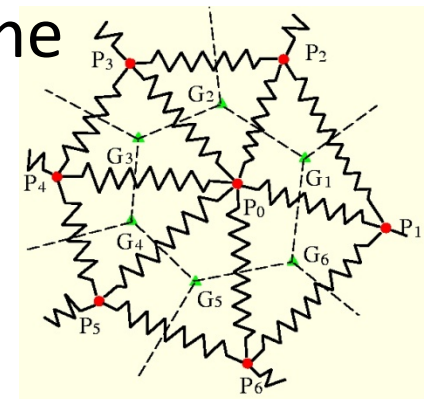
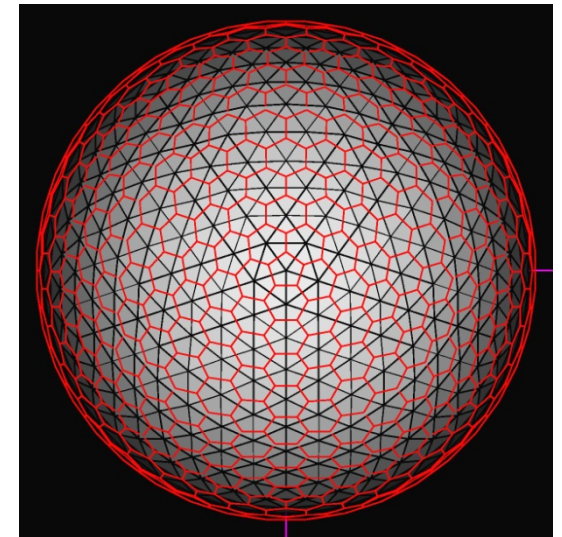
- Flux-form conservative nonhydrostatic scheme

Split-explicit time integration

Mass, total energy & momentum conserving

Satoh (2002, *Mon. Wea. Rev.*)

Satoh (2003, *Mon. Wea. Rev.*)



Model description

■ Dynamics

governing equations	Fully compressible non-hydrostatic system
spatial discretization	Finite Volume Method
horizontal grid configuration	Icosahedral grid
vertical grid configuration	Lorenz grid
topography	Terrain-following coordinate
conservation	Total mass, total energy
temporal scheme	Slow mode — explicit scheme (RK2, RK3) Fast mode — Horizontal Explicit Vertical Implicit scheme

■ Physics

radiation	MSTRNX / MSTRNX-AR5 (Sekiguchi and Nakajima, 2008)
cloud physics	Grabowski(1998) ; NSW6 (Tomita 2008); NDW6 (Seiki 2009)
shallow clouds boundary layer	MY level 2 (Mellor and Yamada 1982; Noda et al. 2010) MYNN level 2.5 or 3 (Nakanishi and Niino 2006)
surface flux	Louis(1979), Uno et al.(1995)
surface processes	SST specified & bucket / slab ocean & MATSIRO

MJO/ISV Simulations with NICAM

2006 boreal Winter MJO hindcasts

Horizontal grid spacing: **14 km, 7 km, 3.5 km**

Vertical domain:

0 m ~ 38,000 m 40-levels (stretching grid)

Integration:

7km, 14km runs: 30 days from 1 Nov 2006

7km, 14km runs: 30 days from 15 Dec 2006

3.5km run: 7 days from 25 Dec 2006

Initial conditions:

Interpolated from **NCEP final analysis**

(6 hourly, 1.0x1.0 degree grids)

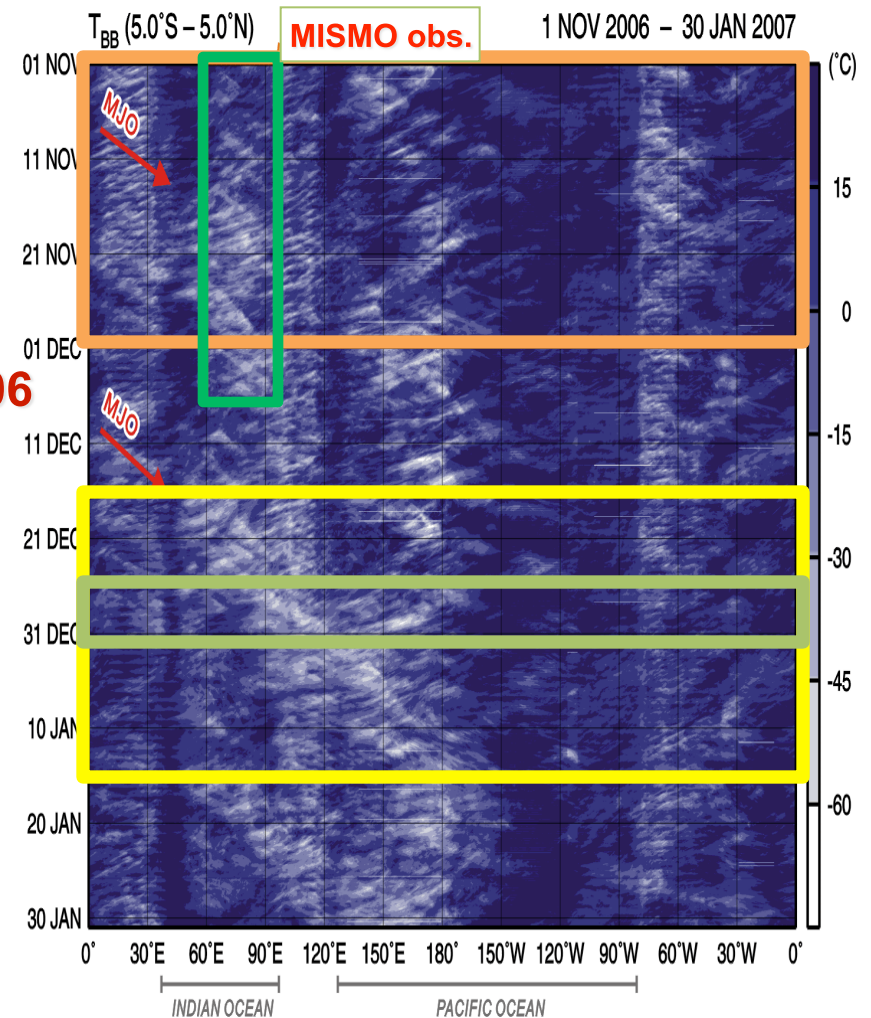
Boundary conditions:

Reynolds SST, Sea ICE (weekly data)

ETOPO-5 topography

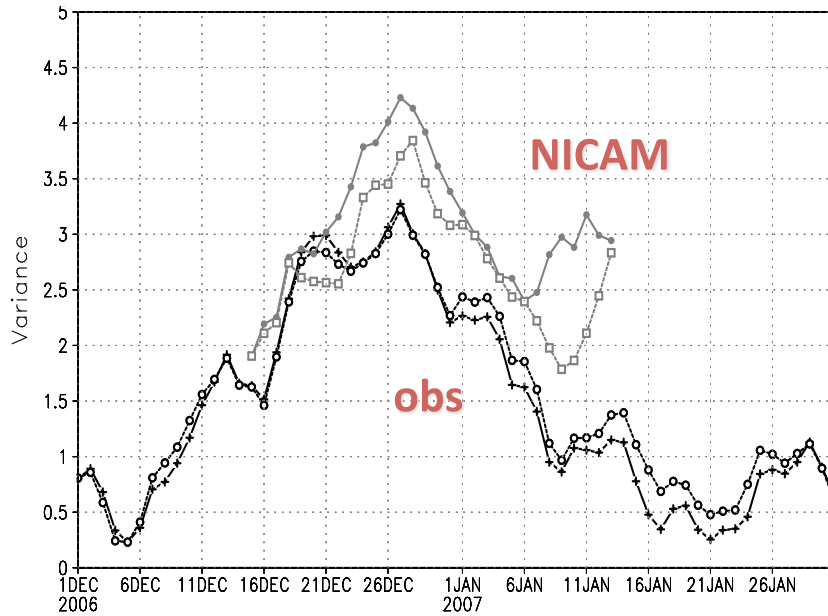
Matthews vegetation

UGAMP ozone climatology (for AMPI2)



- **EXP. Dec 2006: Miura et al.(2007,Science), Nasuno et al.(2009,JMSJ), Sato et al. (2009, J.Clim)**
- **Liu et al. (2009, MWR), Fudeyasu et al. (2009, GRL)**
- **EXP. Nov. 2006 (MISMO): Miura et al. (2009, GRL)**

MJO index



Phase diagram

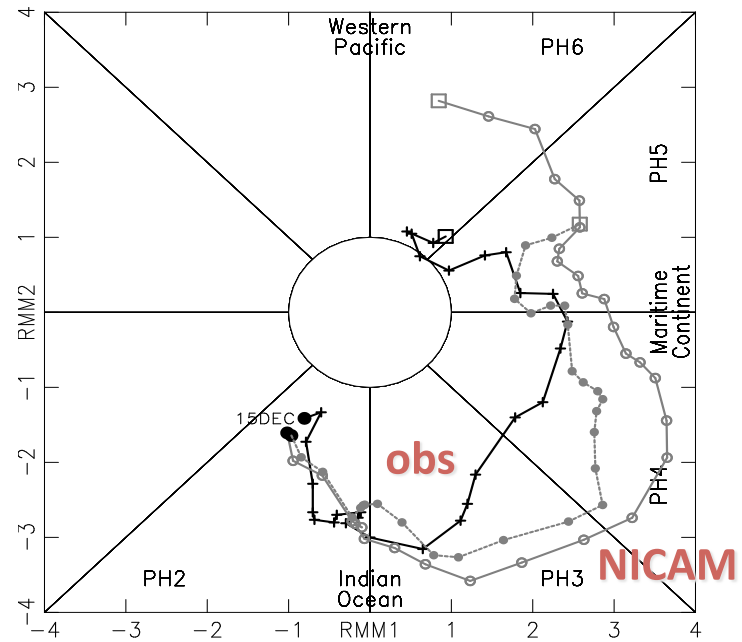
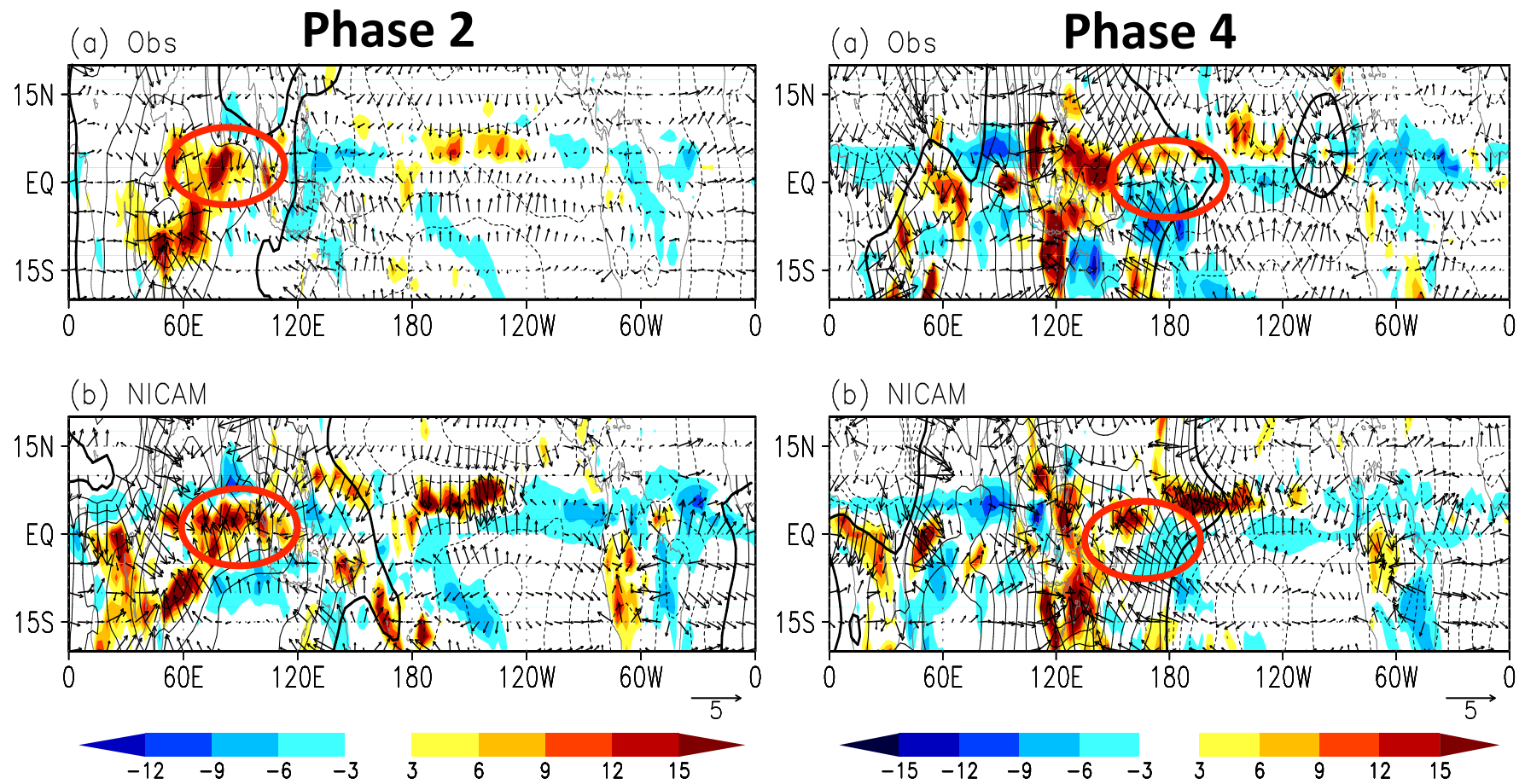


Fig. 3 Evolution of the MJO event in amplitude represented by $(RMM1^2 + RMM2^2)^{1/2}$. The black-solid curve is derived using the anomalous fields described in WH04; others use simple anomalies by excluding the observed climatology for observations (black-dashed), the 14-km NICAM (gray-solid), and the 7-km NICAM (gray-dashed).

Fig. 4 RMM diagram for the MJO event in observations (black-solid), the 14-km NICAM (gray-solid) and the 7-km NICAM (gray-dashed).

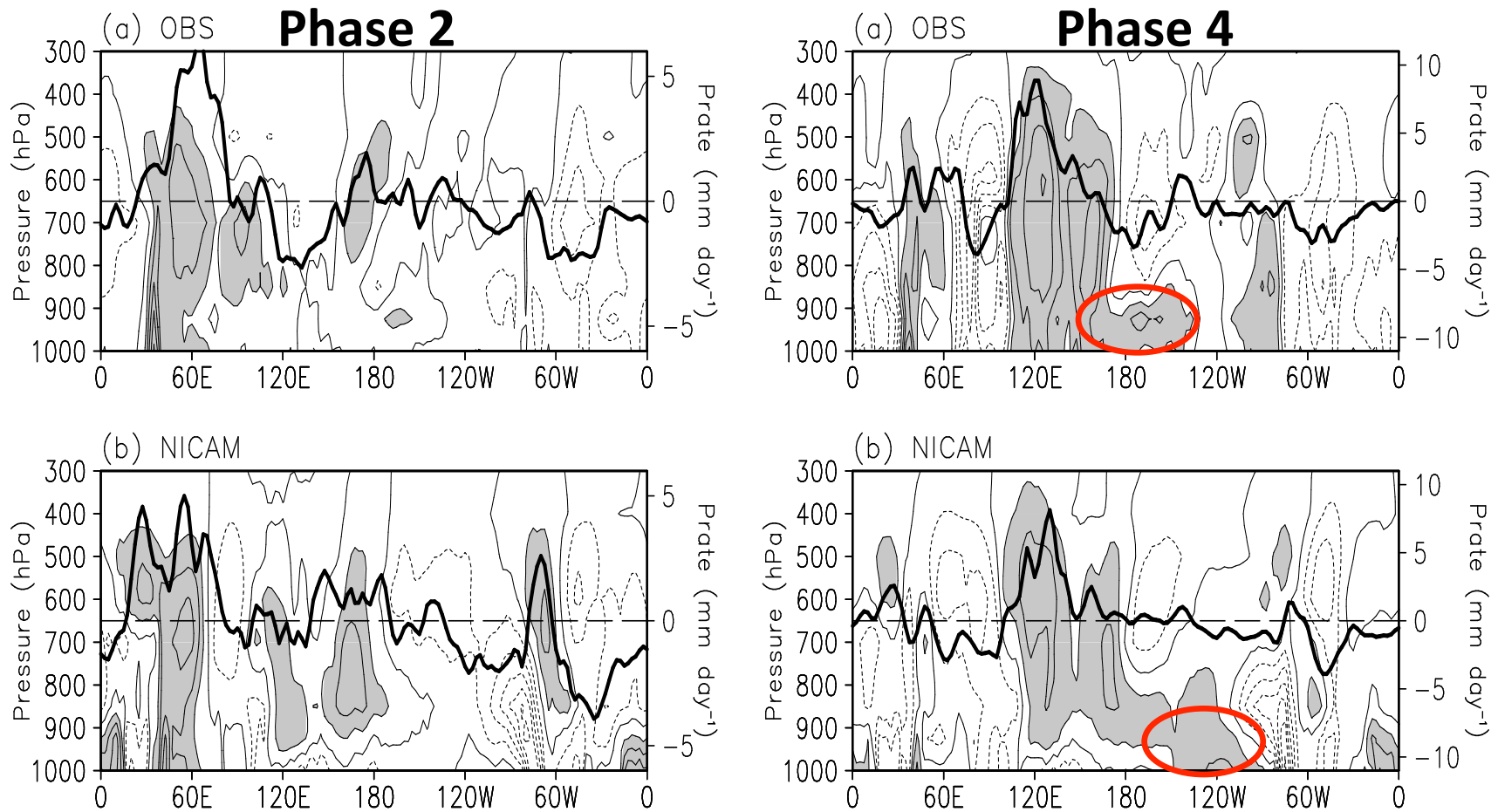
Liu, et al. (2009), Mon. Wea. Rev.



Color: precipitation, contour: divergent wind (925hPa)

Fig. 5 Composites anomalies for Phase 2 of the MJO event in observations (a), and the 7-km NICAM (b). Contours represent the velocity potential (interval is $1 \times 10^6 \text{ m}^2 \text{ s}^{-2}$ with thick-black as 0) at 925 hPa and vectors for the divergent wind at this level. The shading represents the precipitation rate (mm day^{-1}) from the TRMM (a) and NICAM (b).

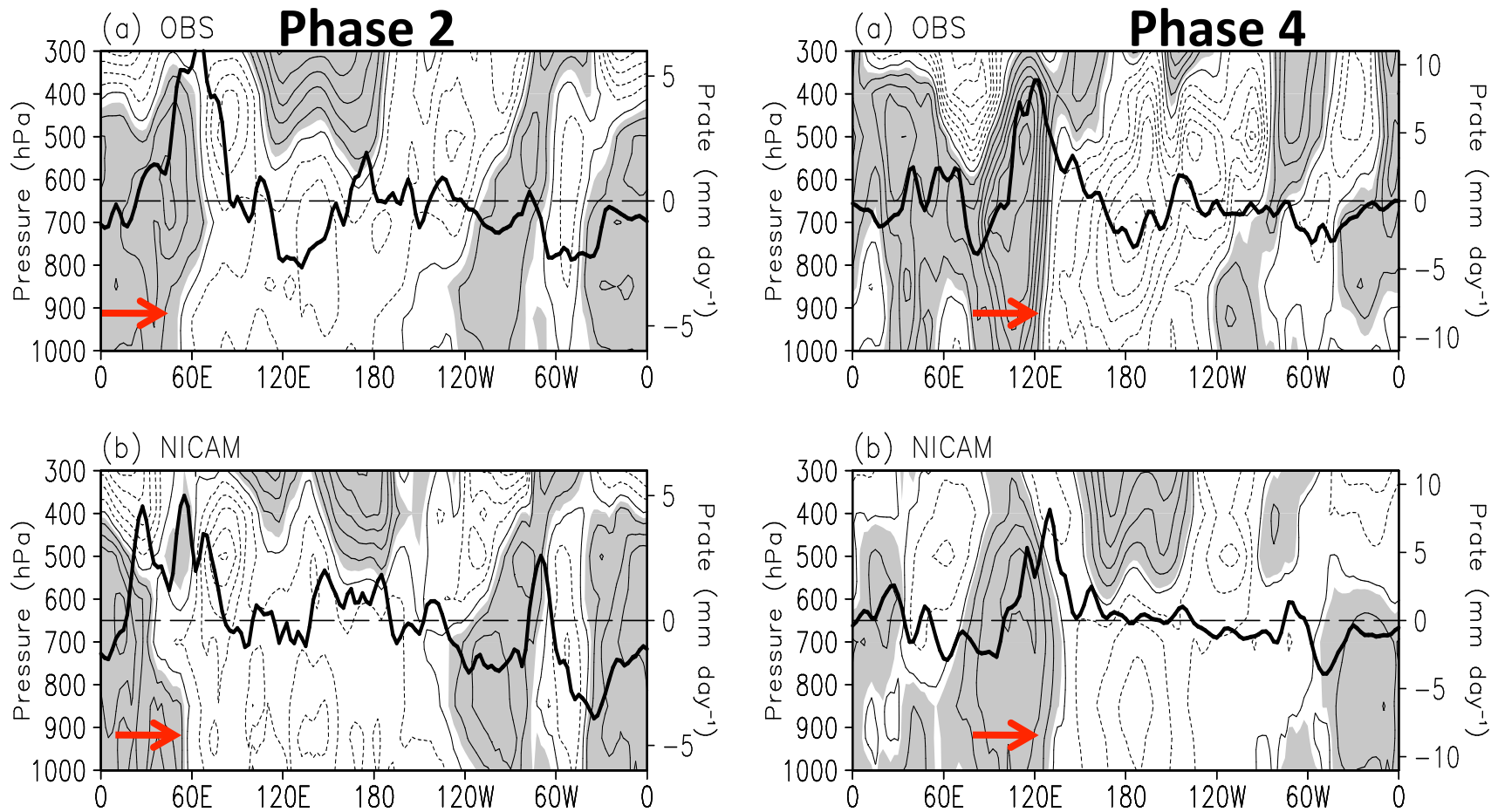
Vertical structure of Specific Humidity



Contour: precipitation

Fig. 6 Same as Fig. 5 except contours represent the specific humidity (interval 0.5 g kg^{-1}) with shaded values greater than and equal to 0. The thick-black curve is for precipitation rate (mm day^{-1}) in TRMM (a) and NICAM (b). All values are along the equator (averaged between 15°S and 15°N).

Vertical structure of zonal wind



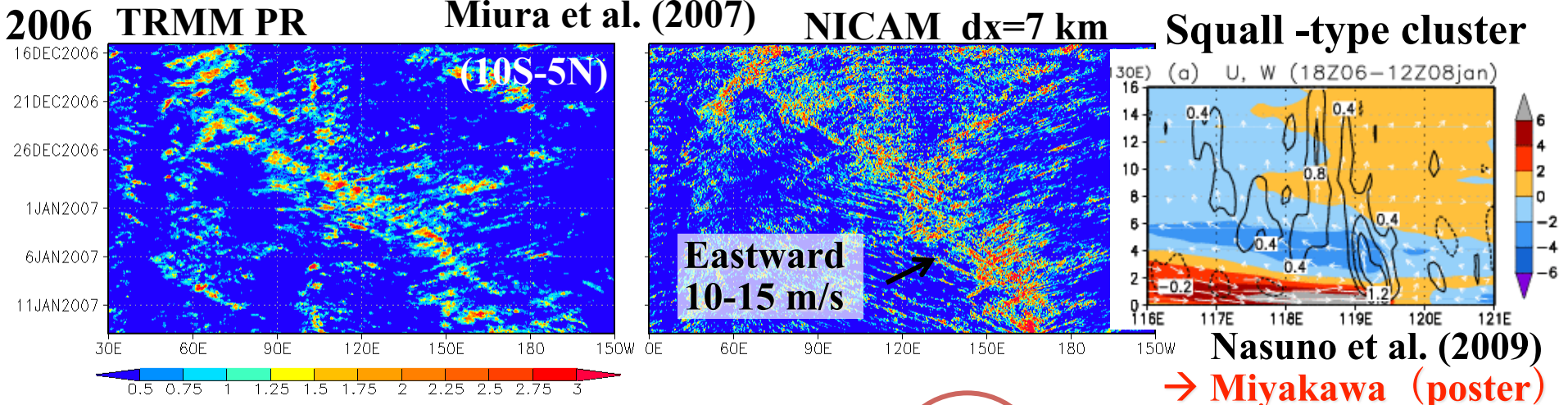
Contour: precipitation

Fig. 7 Same as Fig. 6 except contours represent the zonal wind (interval 0.5 m s⁻¹).

Convective momentum transport (CMT) in MJO

- Moncrieff (2004), Grabowski and Moncrieff (2001), Houze et al. (2000), Oouchi and Yamasaki (2001), Tung and Yanai (2002)

calculation of CMT in a NICAM simulation of an MJO event



Nasuno et al. (2009)
→ Miyakawa (poster)

$$\frac{\partial \bar{u}}{\partial t} = -\bar{u} \frac{\partial \bar{u}}{\partial x} - \bar{v} \frac{\partial \bar{u}}{\partial y} - \bar{w} \frac{\partial \bar{u}}{\partial z} - \frac{1}{\bar{\rho}} \left(\frac{\partial \overline{\rho u' u'}}{\partial x} + \frac{\partial \overline{\rho u' v'}}{\partial y} + \frac{\partial \overline{\rho u' w'}}{\partial z} \right) - \frac{1}{\bar{\rho}} \frac{\partial \bar{P}}{\partial x} + f \bar{v} + \bar{F}_x$$

1° mean wind

Subgrid wind

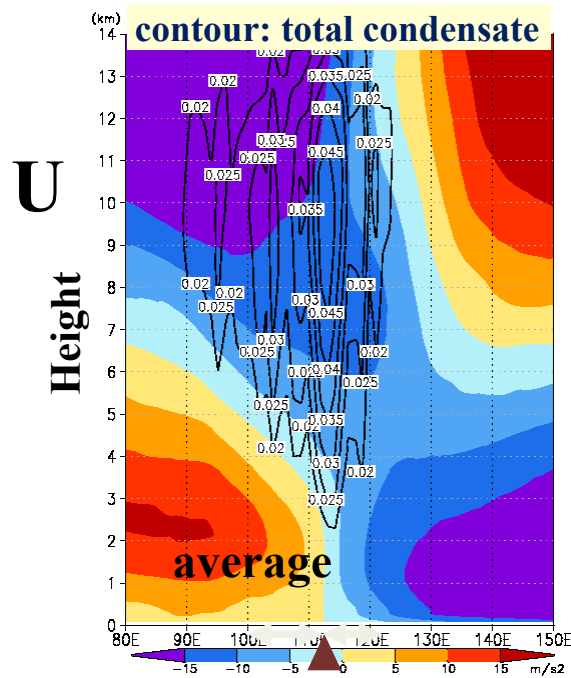
“Convective momentum transport”

Turbulence etc.

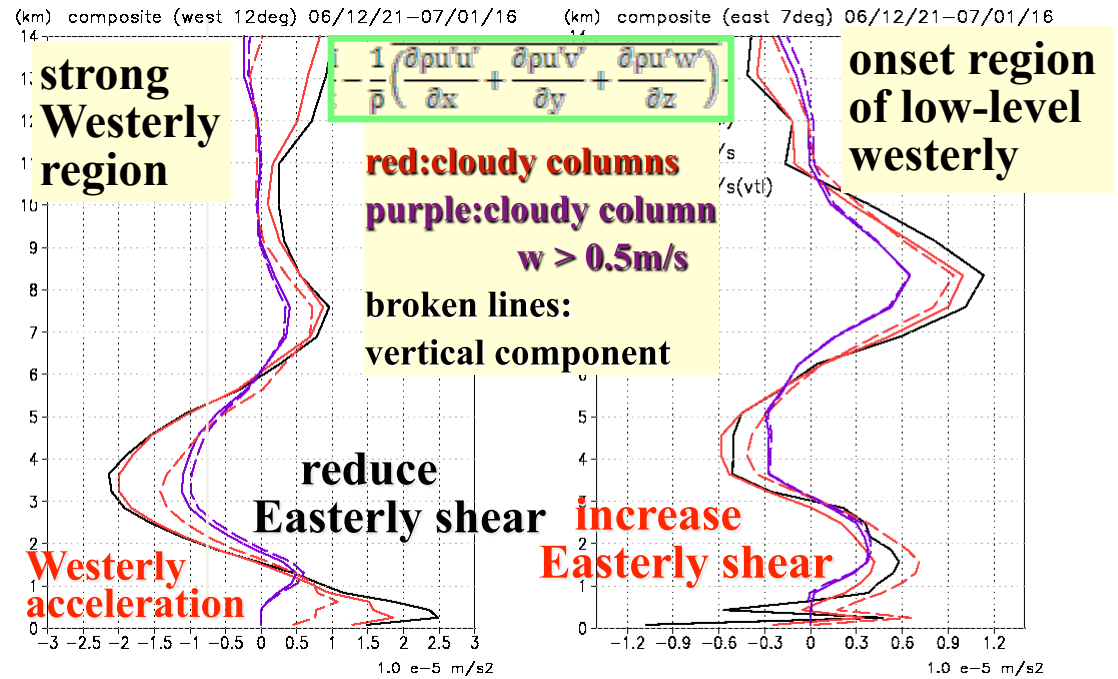
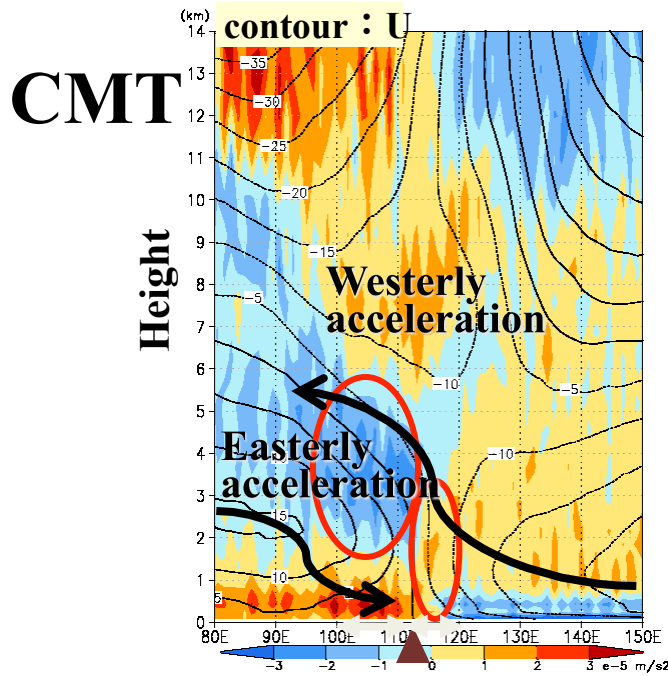
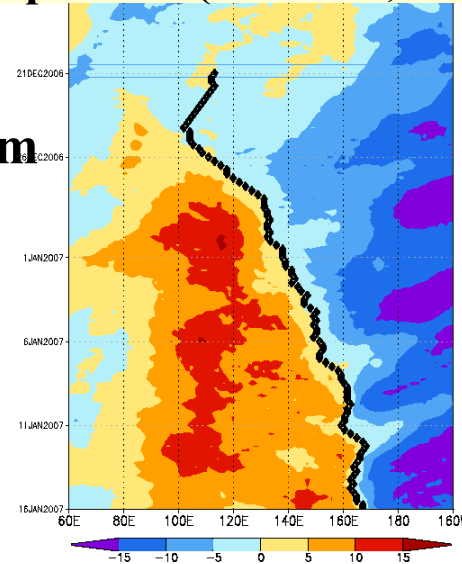
$X = \bar{X} + X'$
 \bar{X} : ~1° mean values
 X' : deviations

composite of U and CMT(10S-5N)

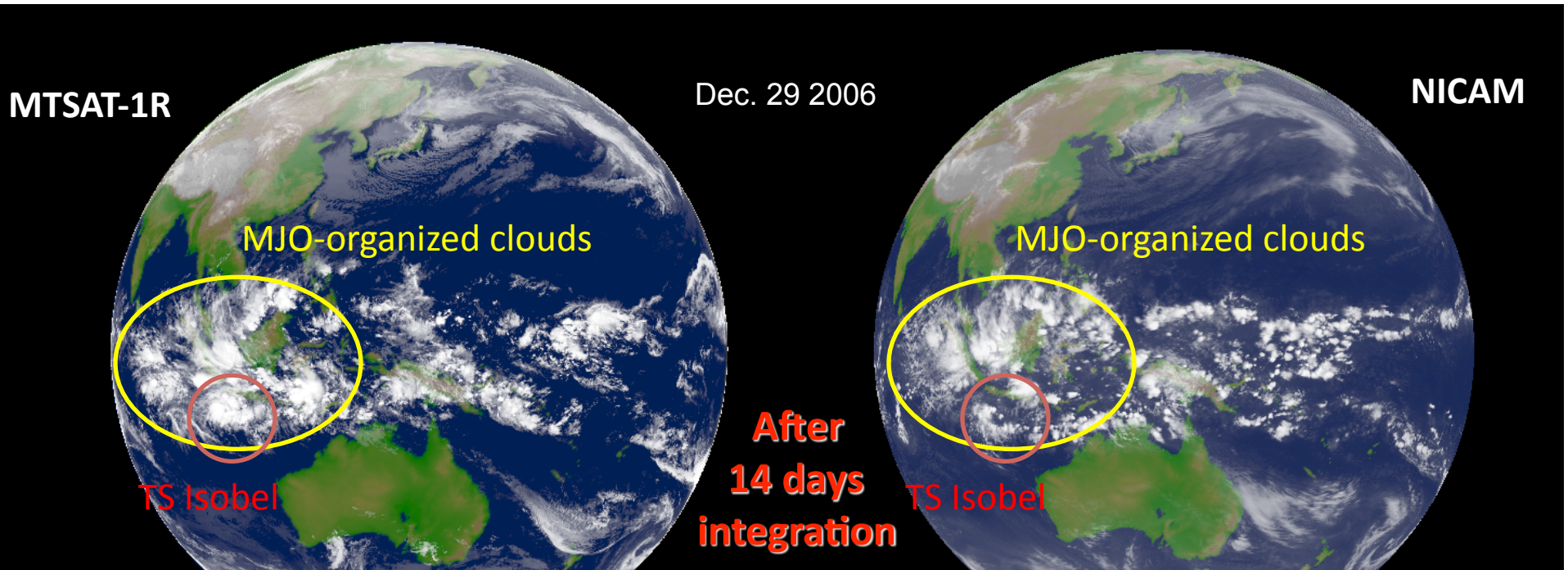
Base point: $U(z=1.5\text{km}, 10\text{S}-5\text{N}) = 0$



U
z=1.5 km

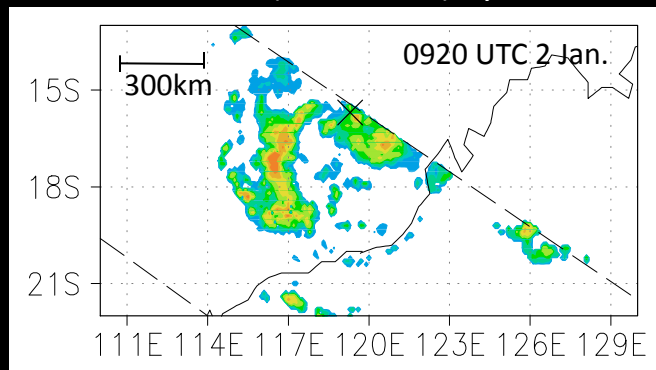


Fudeyasu, H., Wang, Y., Satoh, M., et al. (2008) The global cloud-resolving model NICAM successfully simulated the lifecycles of two real tropical cyclones. Geophys. Res. Lett., 35, L22808.

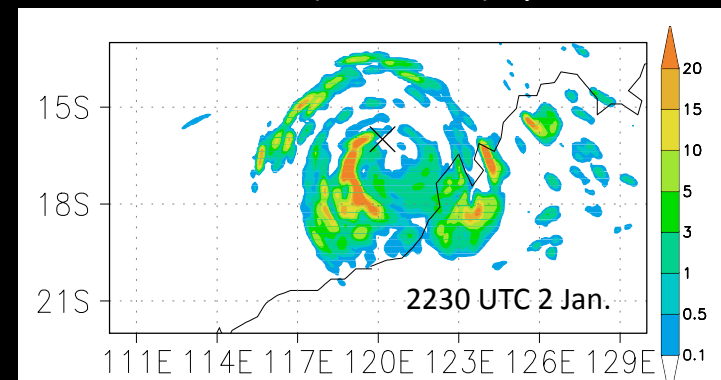


NICAM reasonably produced not only the large-scale circulation, such as the MJO, but also the embedded mesoscale features, such as TC rainbands.

Surface rain rate (mm hour^{-1}) by TRMM-TMI



Surface rain rate (mm hour^{-1}) by NICAM

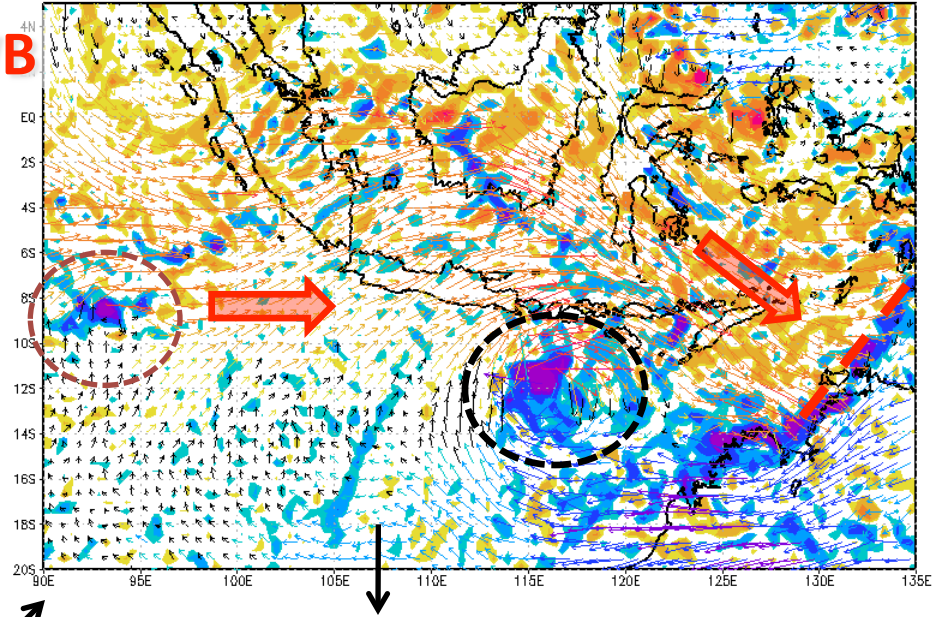
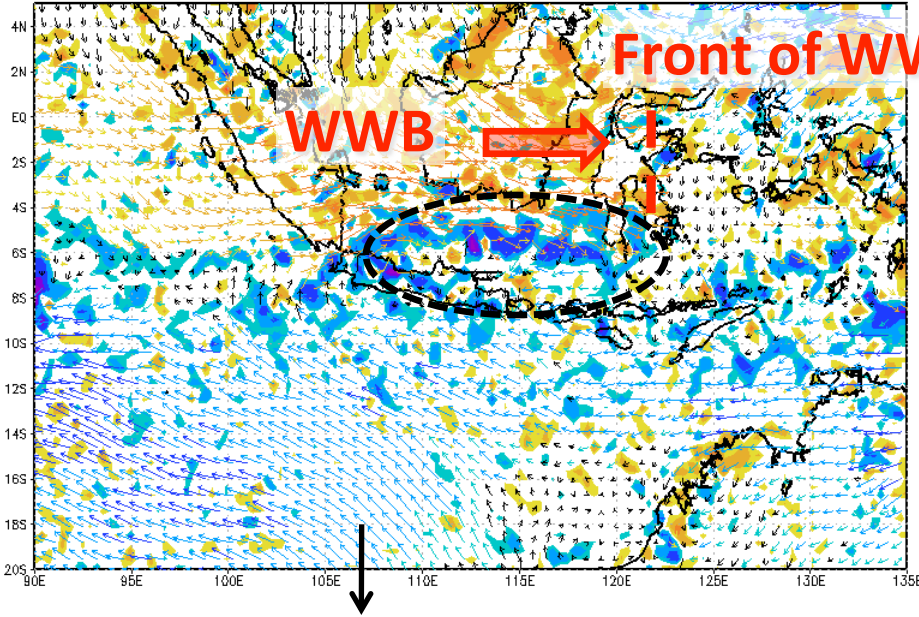


TC genesis in MJO (NICAM 7-km mesh)

Relative vorticity (z=1km)

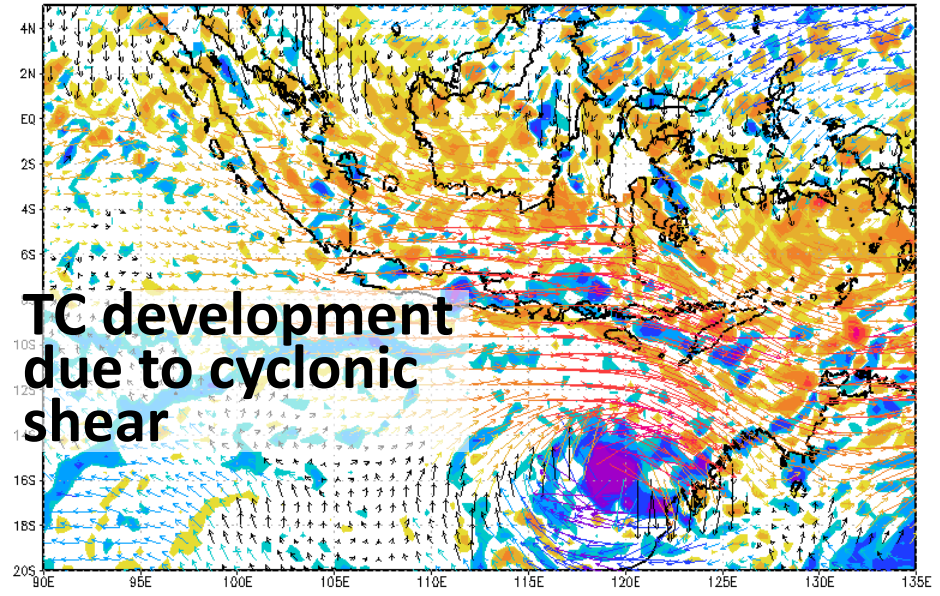
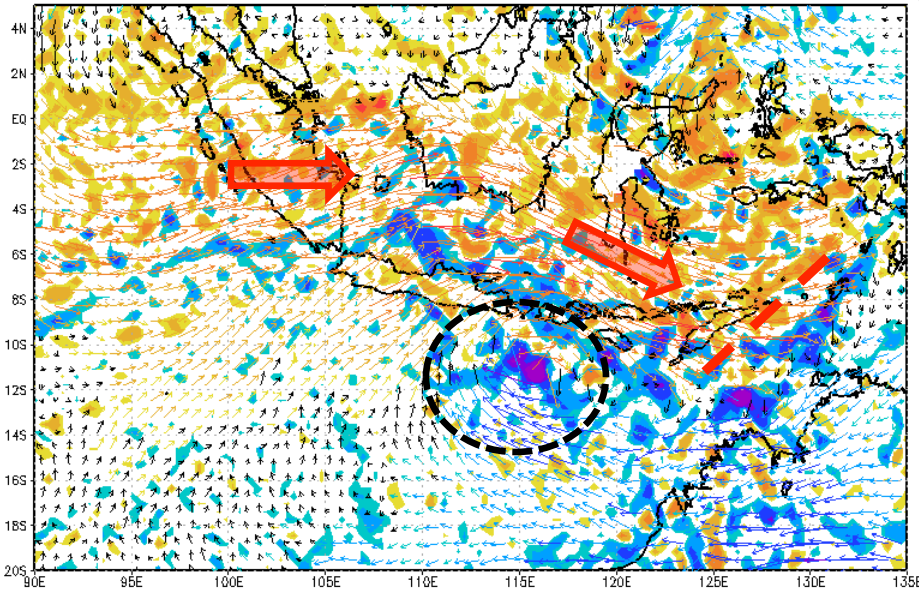
1km-wind(sha=u) rel-vor*10⁵ 12/27/12 T=50

1km-wind(sha=u) rel-vor*10⁵ 12/31/0 T=64

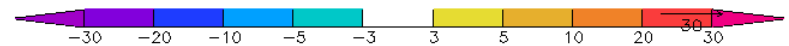
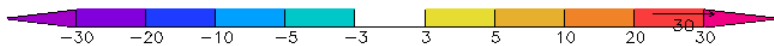


1km-wind(sha=u) rel-vor*10⁵ 12/30/0 T=60

1km-wind(sh=u) rel-vor*10⁵ 01/2/12 T=74



TC development
due to cyclonic
shear



TC Nargis ensemble simulation

Taniguchi et al. (2010), JMSJ special edition on the Myanmar Cyclone, in press

Horizontal mesh size: **14 km**

Vertical mesh size: 0 m ~ 38,000 m
(40 layer, stretching grid)

Integration: **30-days**

Initial condition: http://www.nasa.gov/mission_pages/hurricanes/archives/2008/h2008_nargis.html

linear interpolation from **JMA GPV/GSM data** (every 6hr, 0.5x0.5grid)

initial time: **1200UTC, 10, 23, 24, 25, 26, 27, 28, Apr 2008**

(7 control run without any perturbation:

Lagged Average Forecasting (LAF) method, Hoffman and Kalnay, 1993)

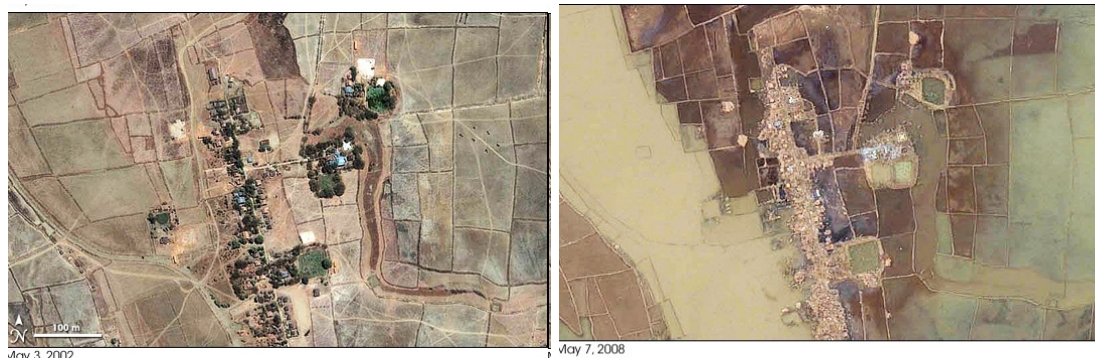
without any nudging process (Nargis formed on **27 Apr 2008**)

Boundary condition:

weekly Reynolds-SST , Sea ICE

ETOPO-5 topography, Matthews vegetation

UGAMP ozone climatology (AMIP2)

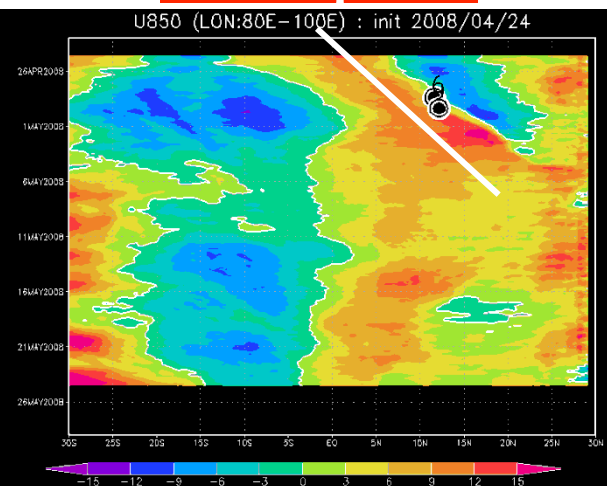
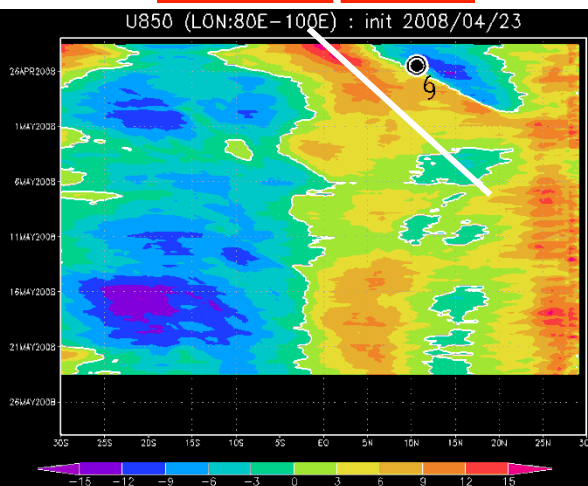
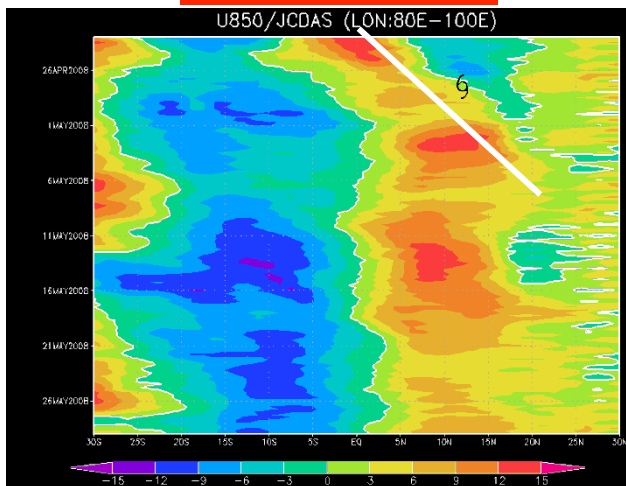


U850 (Averaged: 80E-100E)

Obs.

Init. Apr 23

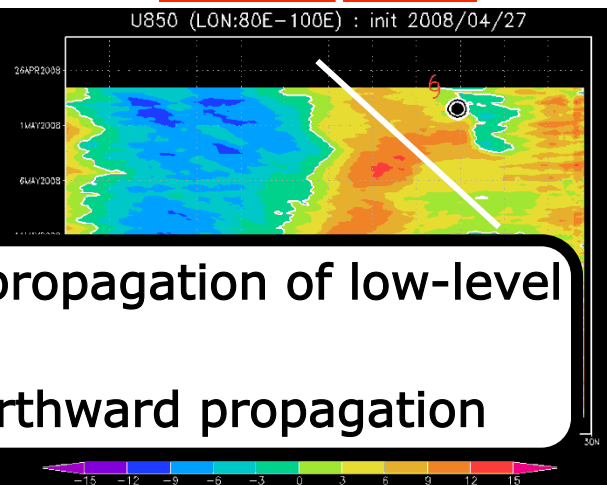
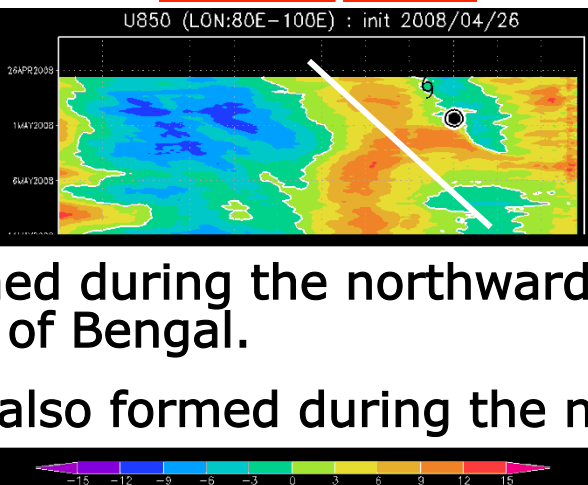
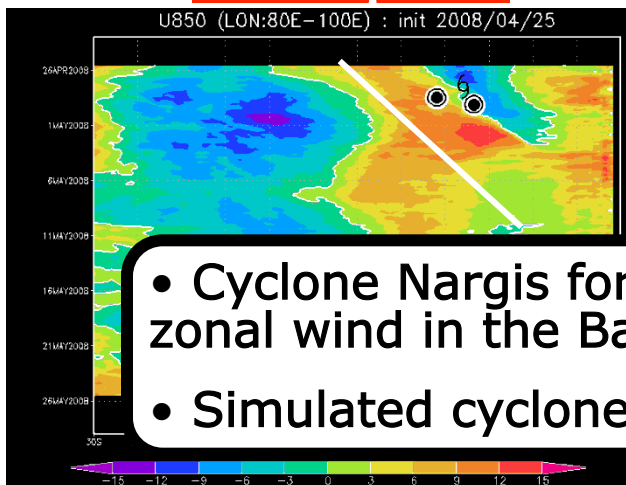
Init. Apr 24



Init. Apr 25

Init. Apr 26

Init. Apr 27



- Cyclone Nargis formed during the northward propagation of low-level zonal wind in the Bay of Bengal.
- Simulated cyclones also formed during the northward propagation

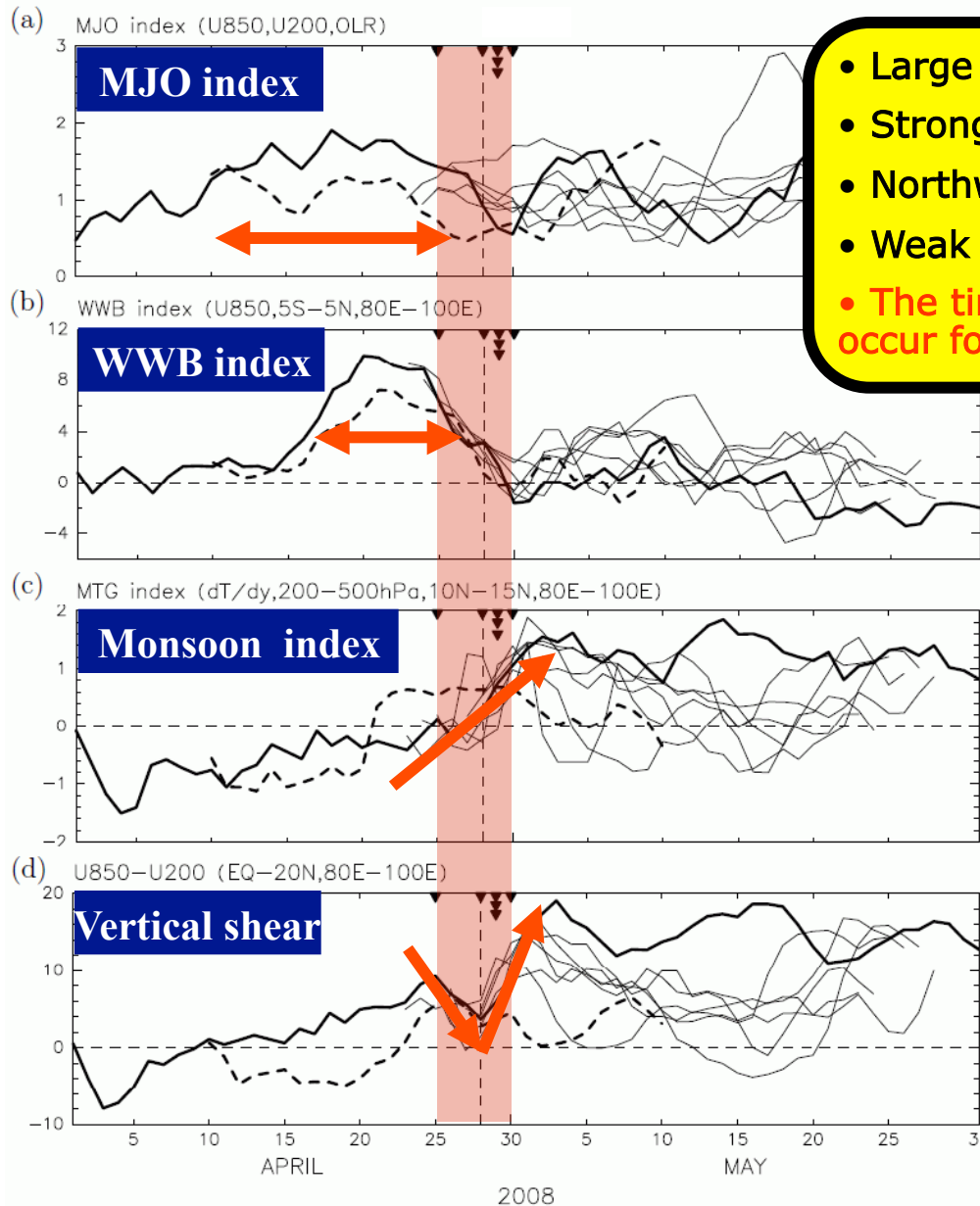
6

Loc. of TC genesis (Obs.)

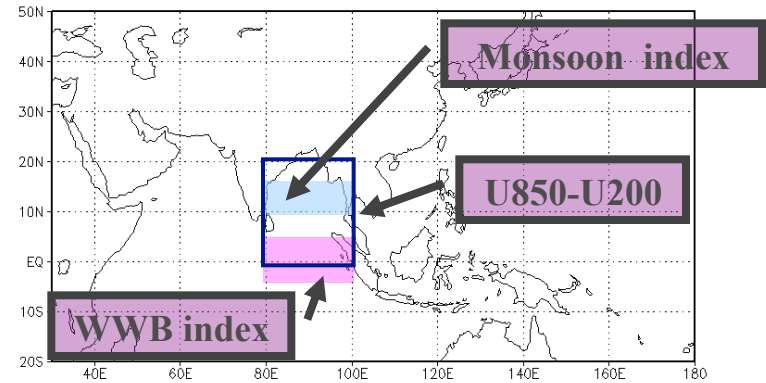
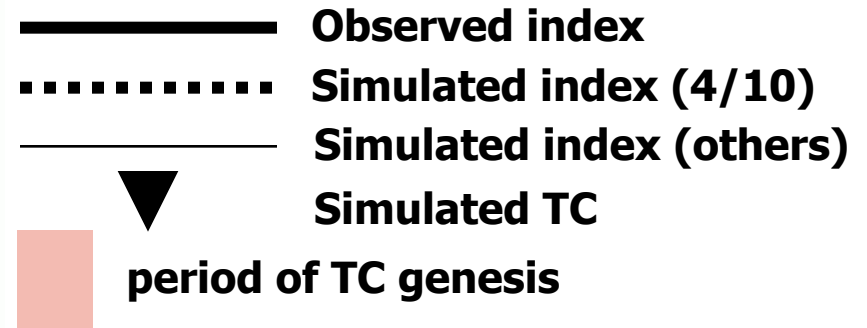


Loc. of TC genesis (Sim.)

(a) MJO index, (b) WWB index, (c) MTG index, (d) Vertical shear

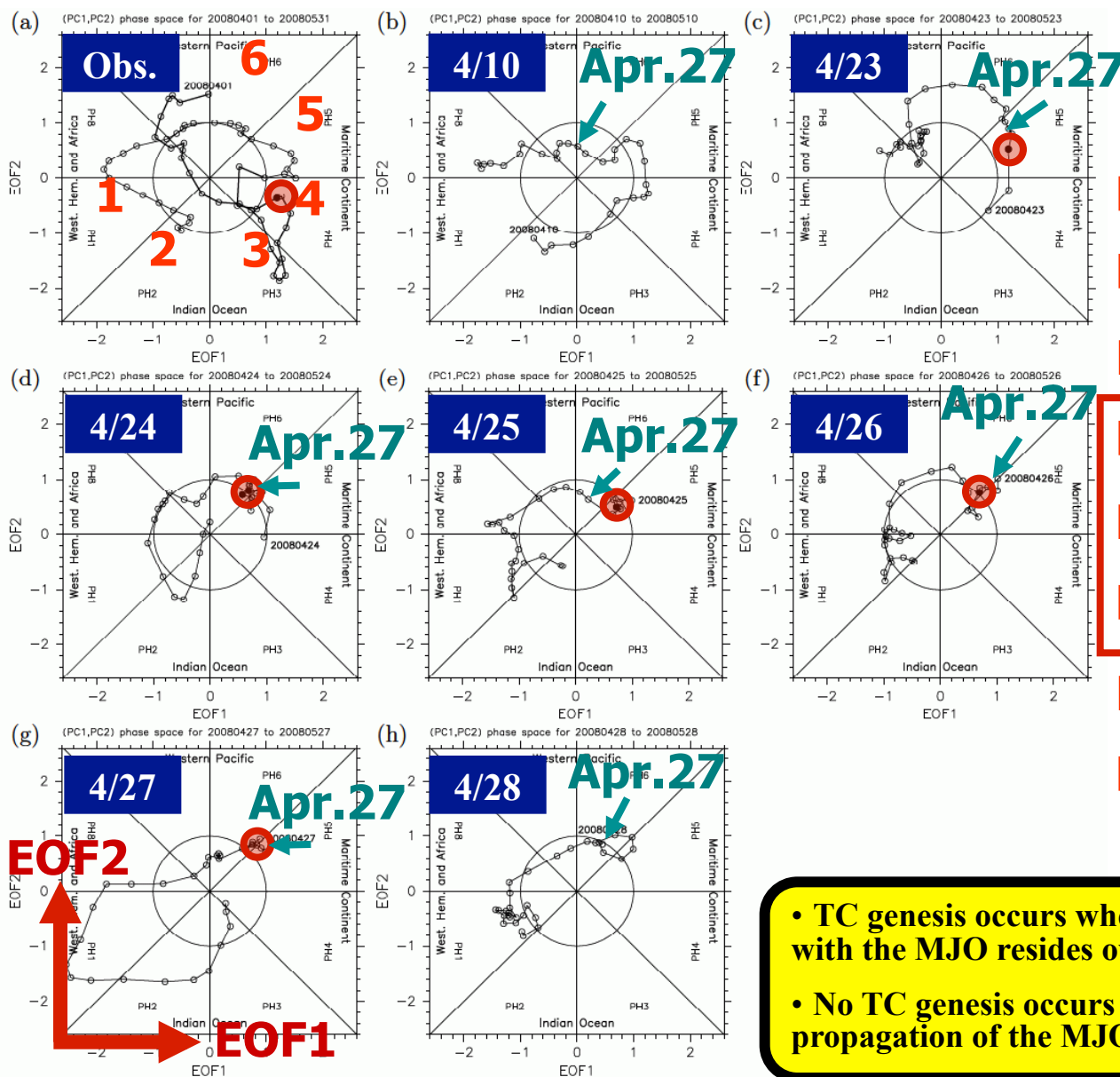


- Large amp. before TC genesis (MJO)
- Strong wind in BoB before TC genesis (WWB)
- Northward migration of the area of westerly in BoB
- Weak vertical shear before TC genesis
- The timing of Monsoon onset is earlier or does not occur for the case with initial day of Apr. 10.

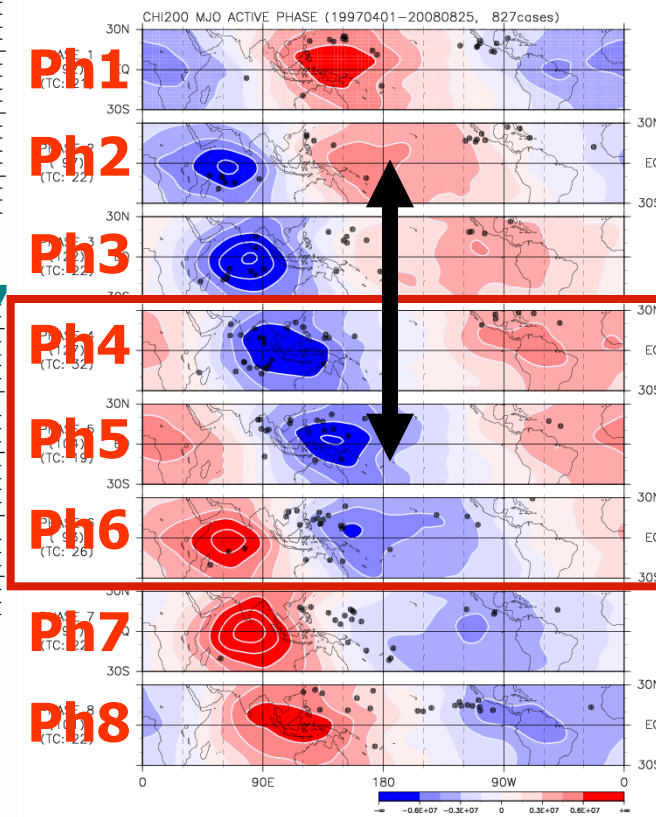


MJO phase: (a) observed, (b-h) simulated

 TC genesis



CHI200 composite on each MJO phase

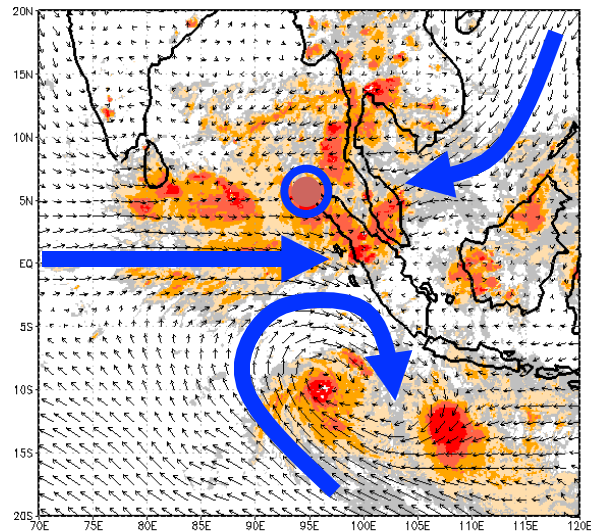


- TC genesis occurs when active convective region associated with the MJO resides over the maritime continent region.
- No TC genesis occurs for the member of which phase propagation of the MJO is not reproduced.

Incipient disturbances for cyclone Nargis: U10m & OLR (IR)

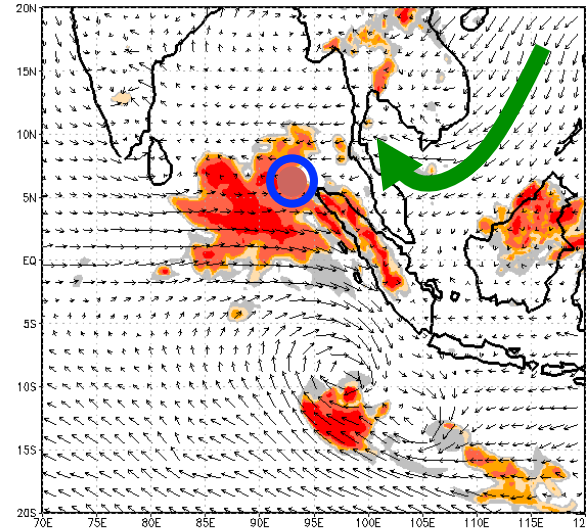
Obs.

12Z23APR2008



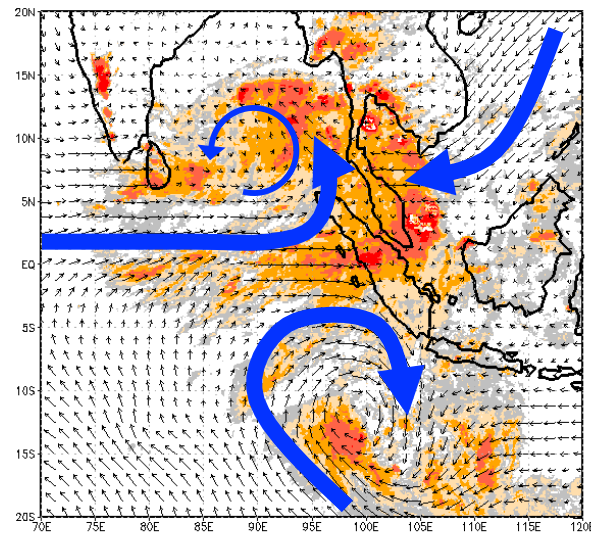
NICAM : 4/23

13Z23APR2008

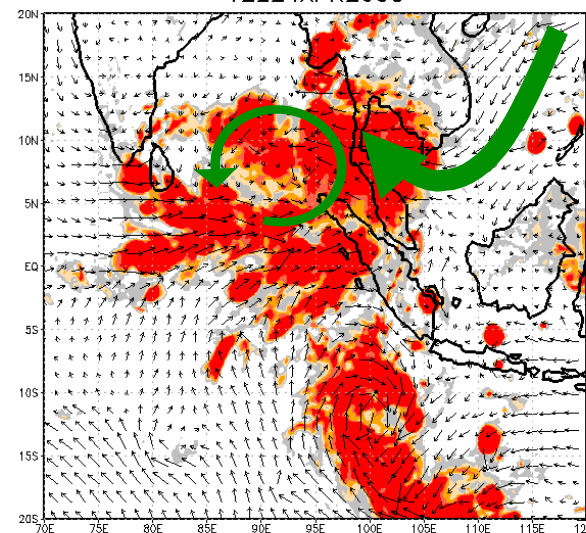


- **WWB**
- **Cyclonic eddy in SIO**
- **Wind from the South China Sea**
- **A weak cyclonic circulation**

12Z24APR2008



12Z24APR2008



- **Northward migration of WWB**
- **Cyclonic eddy in NIO**
- **Wind from the South China Sea**

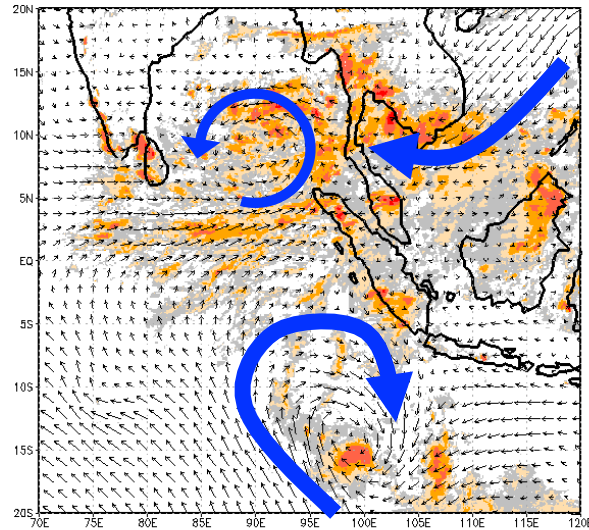
20

20

Incipient disturbances for cyclone Nargis

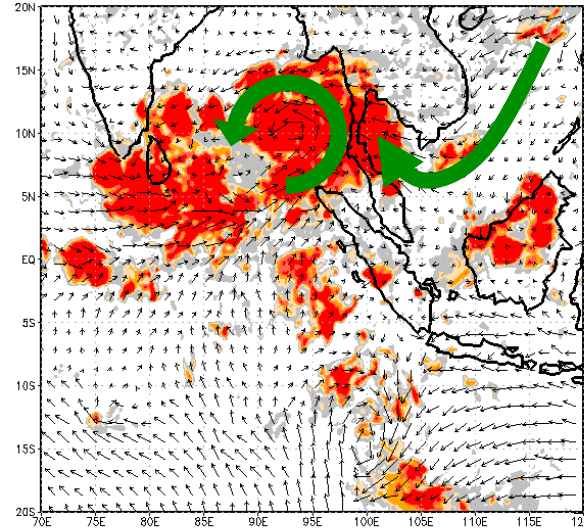
Obs.

12Z25APR2008



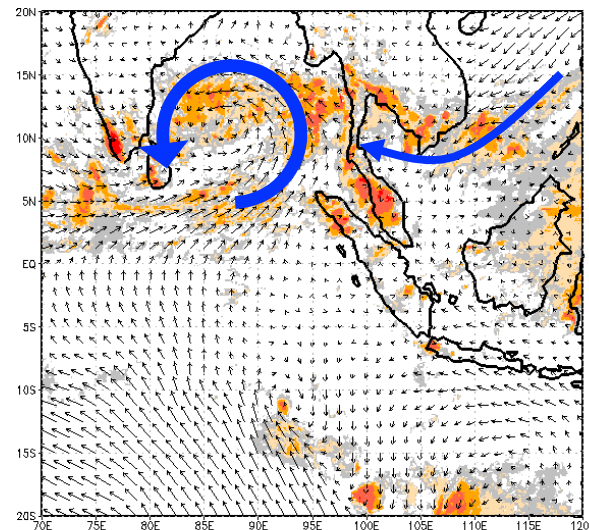
NICAM : 4/23

12Z25APR2008

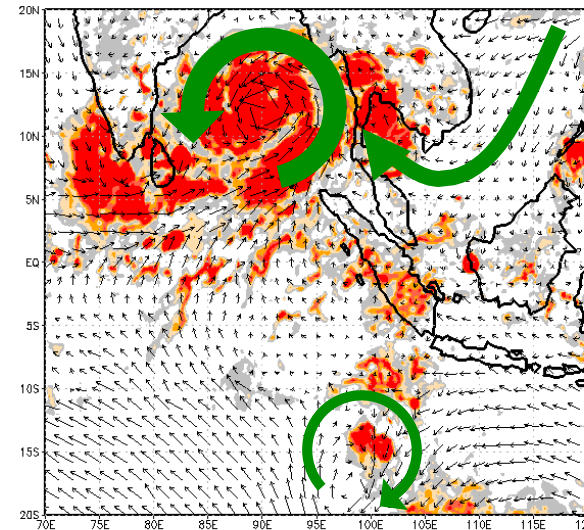


- Northward migration of Cyclonic eddy in NIO
- Wind from the South China Sea

12Z26APR2008



12Z26APR2008

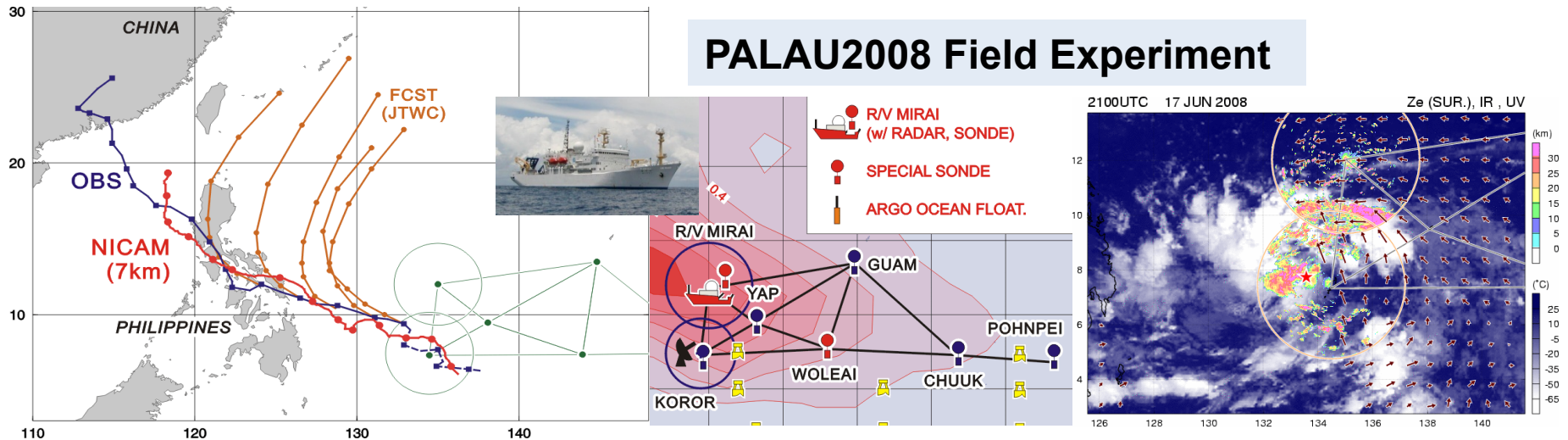


- Northward migration of Cyclonic eddy in NIO
- northward movement of northern vortex and its cyclonic circulation development

20 →

20 →

TC Fengshen simulation



Horizontal grid spacing: **14 km, 3.5 km**

Vertical domain: 0 m ~ 38,000 m (40-levels)

Integration: **7 days integration just finished**
10 (7) days from 00UTC 15 Jun 2008

Initial conditions:

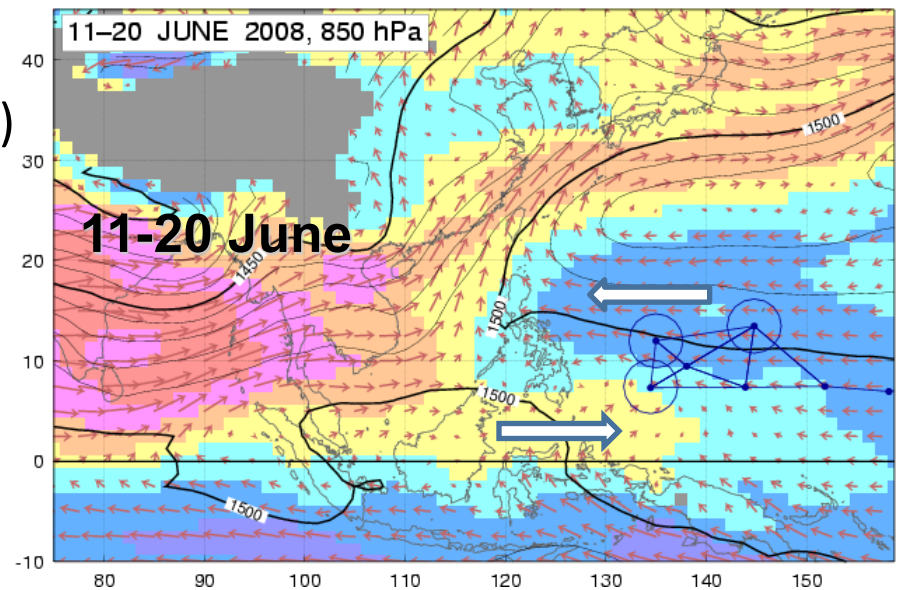
ECMWF YOTC Operational data

NCEP final analysis (land surface, SST)

Boundary conditions:

slab ocean (nudging to Reynolds weekly SST)

--- Fengshen formed on **17 Jun 2008**



Onset of Western Pacific Monsoon & Weak MJO → equatorial westerly

2. MJO activity

Compared to the very strong MJO activity of DJF 2007/08, MJO activity during YOTC has been weaker.

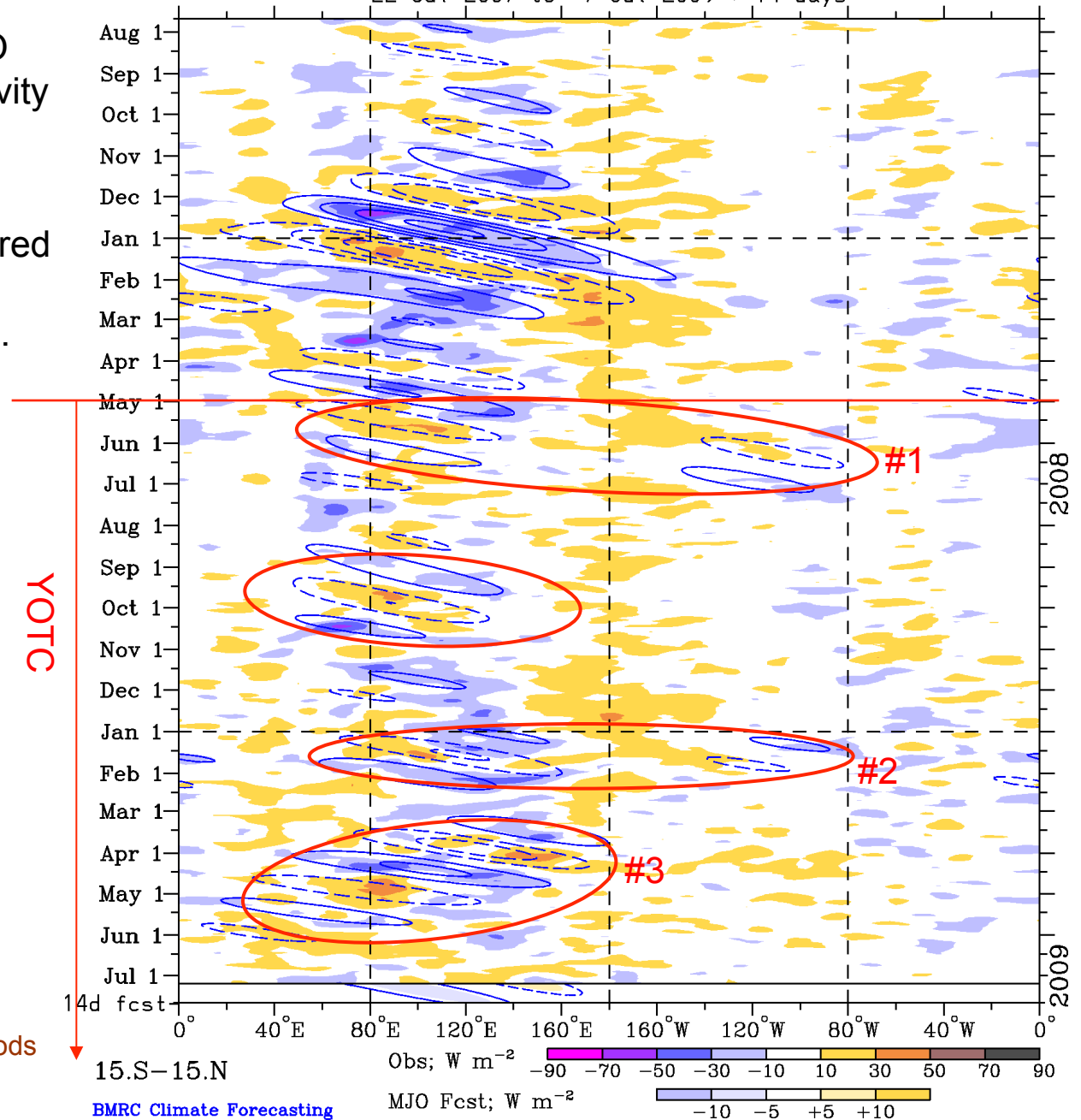
Nevertheless, important and interesting MJO activity still occurred in **May-Jun 2008**, **Sept-Oct 2008**, **Jan-Feb 2009**, and **Mar-Jun 2009**.

So far, the MJO activity centred on **April 2009** has been the strongest (using multiple measures).

Note also the tendency for suppressed convection near and to the east of the date line during much of the YOTC period (i.e. weak La Nina).

“MJO” defined in this plot through filtering of OLR anomalies for eastward waves 1-5, periods 30-96 days (Wheeler and Weickmann 2001)

Real-time MJO filtering superimposed upon 7drn R21 OLR Anomalies
 MJO anomalies blue contours, CINT=8. (4. for forecast)
 Negative contours solid, positive dashed
 22-Jul-2007 to 7-Jul-2009 + 14 days

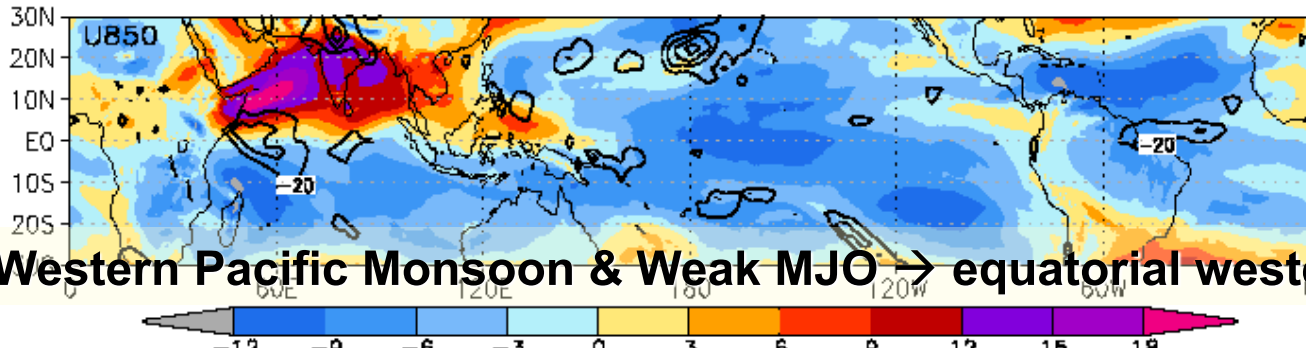


U850

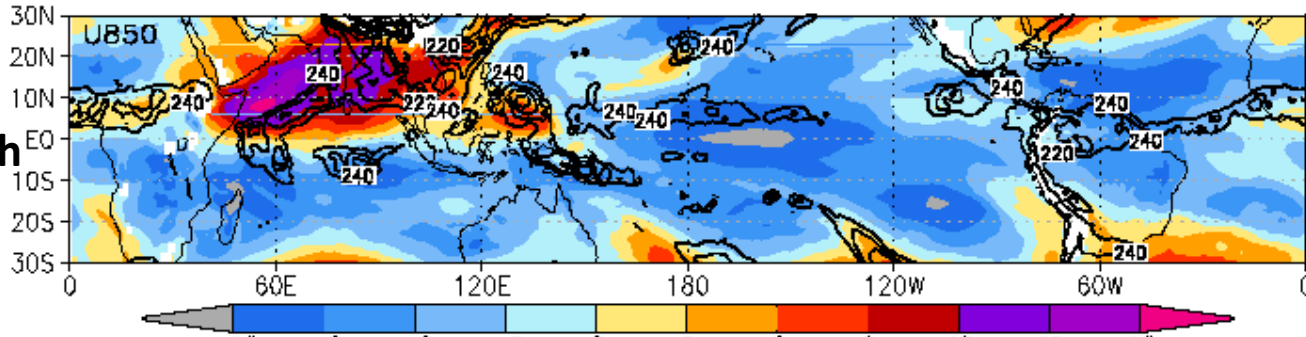
**ECMWF
YOTC**

Onset of Western Pacific Monsoon & Weak MJO → equatorial westerly

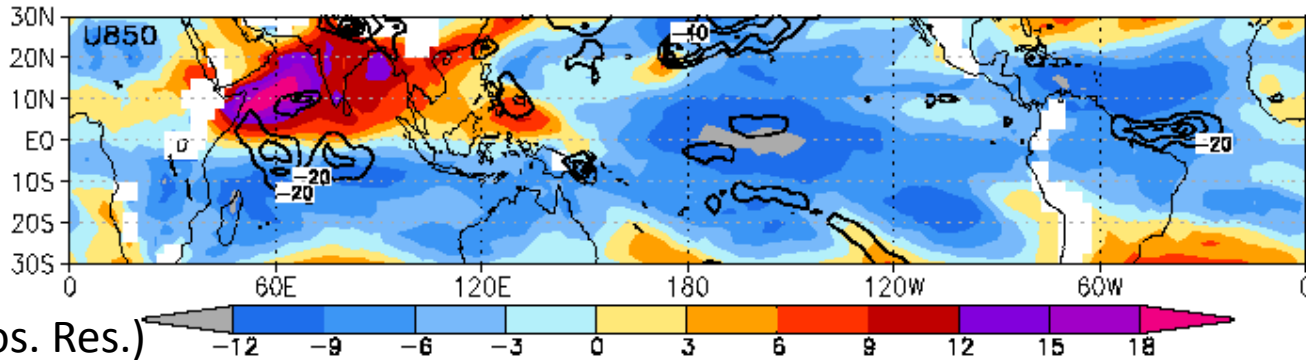
**15-21
June
2008**



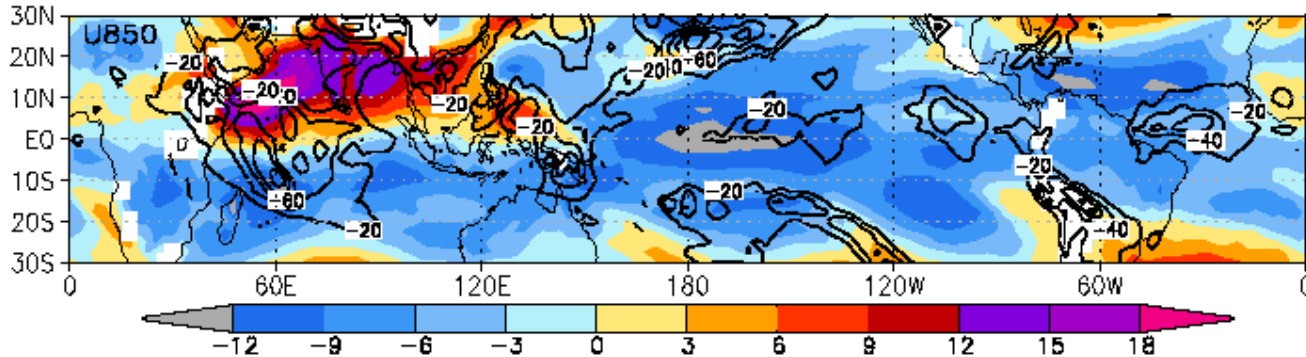
**NICAM
3.5 km mesh**



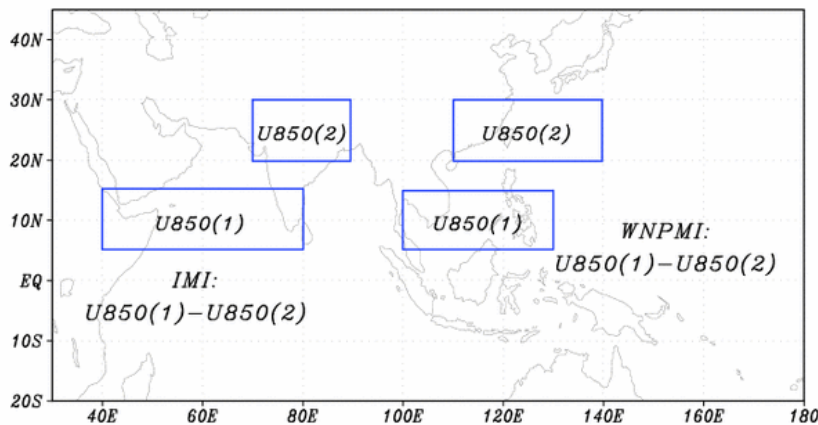
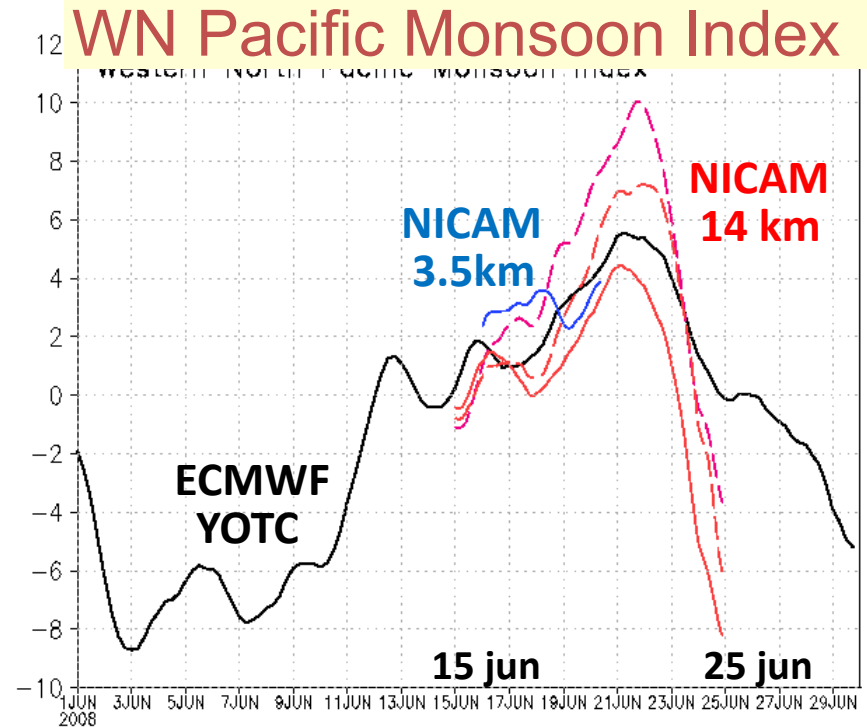
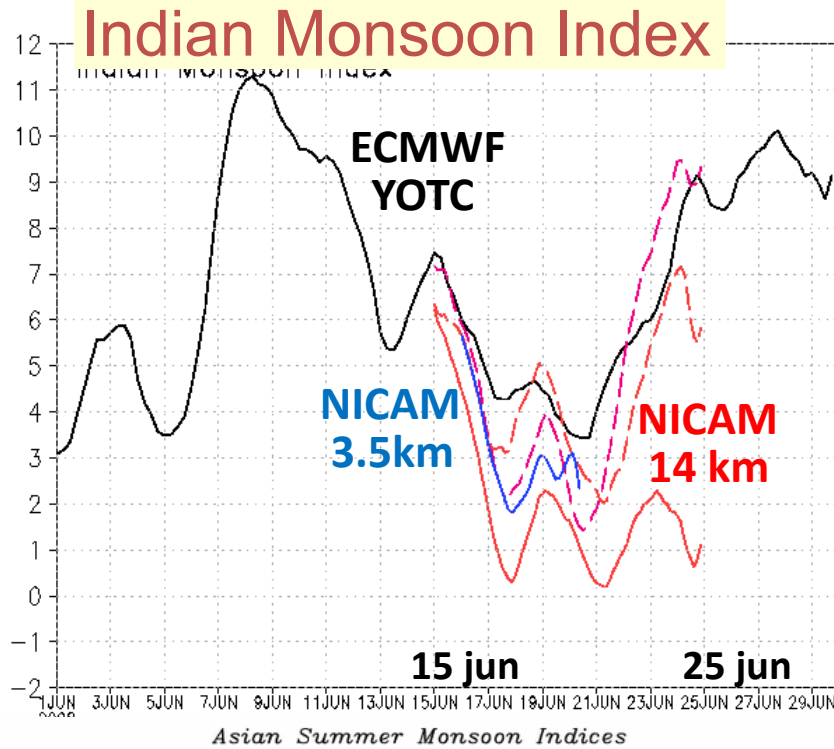
**NICAM
14km mesh
(MY2)
Revised by
Noda et al.**



**NICAM
14km mesh
(MYNN2.5)
not tuned**



Monsoon indices (Jun 2008)

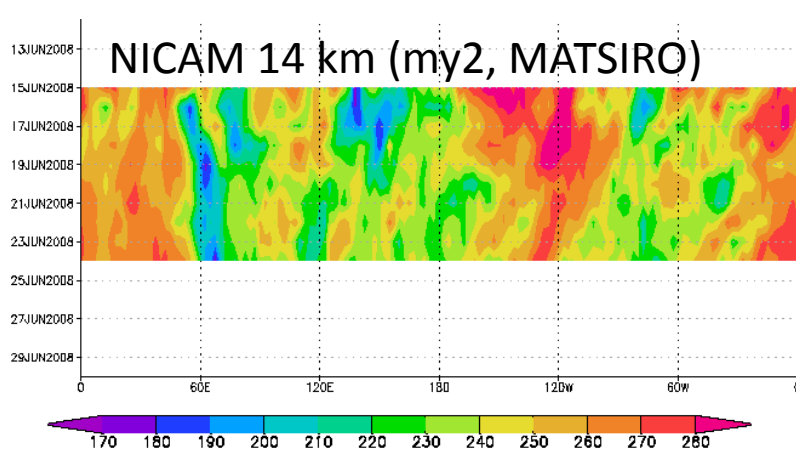
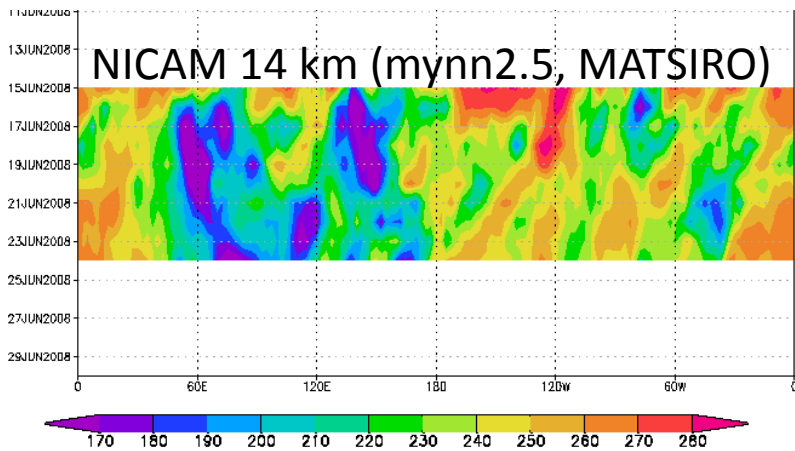
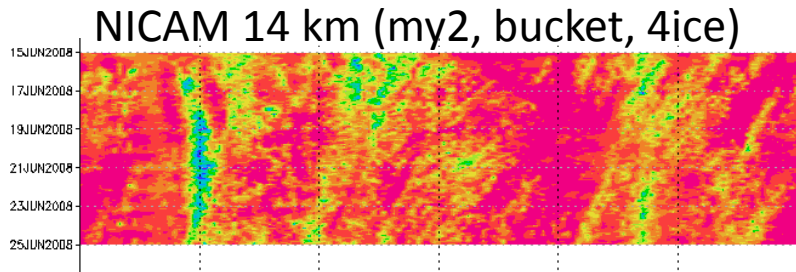
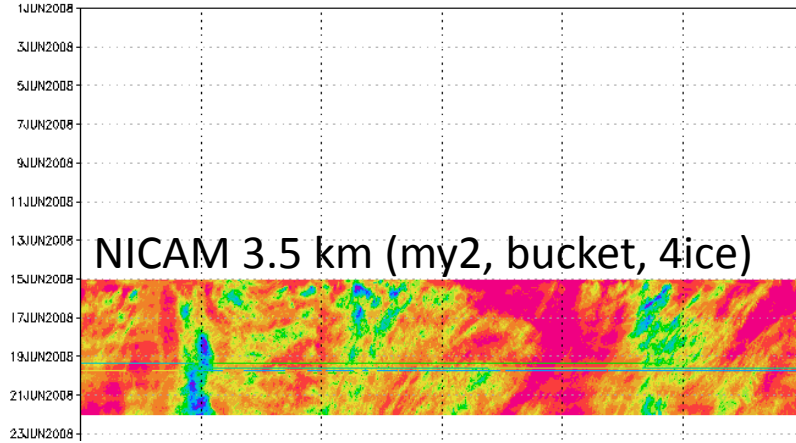
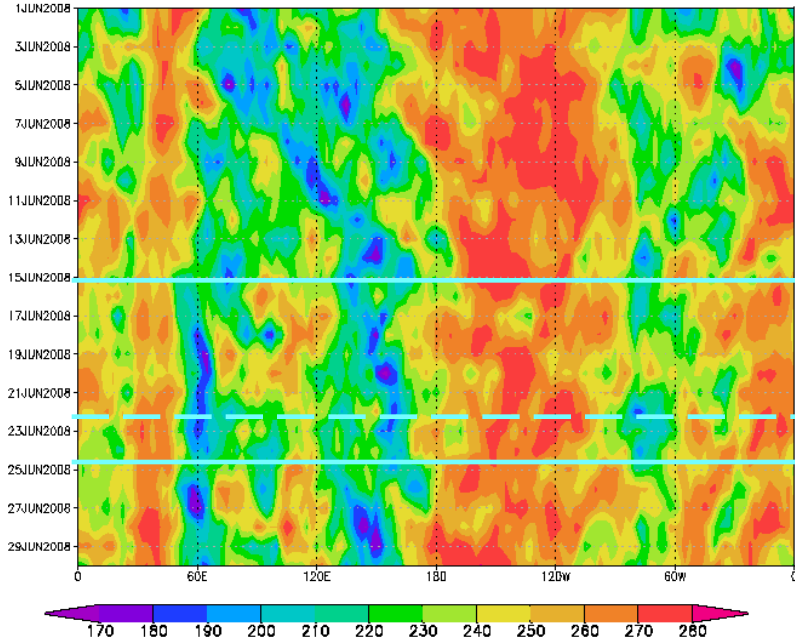


$$\text{IM Index} = U850(40E-80E, 5N-15N) - U850(70E-90E, 20N-30N)$$

$$\text{WNPM Index} = U850(100E-130E, 5N-15N) - U850(110E-140E, 20N-30N)$$

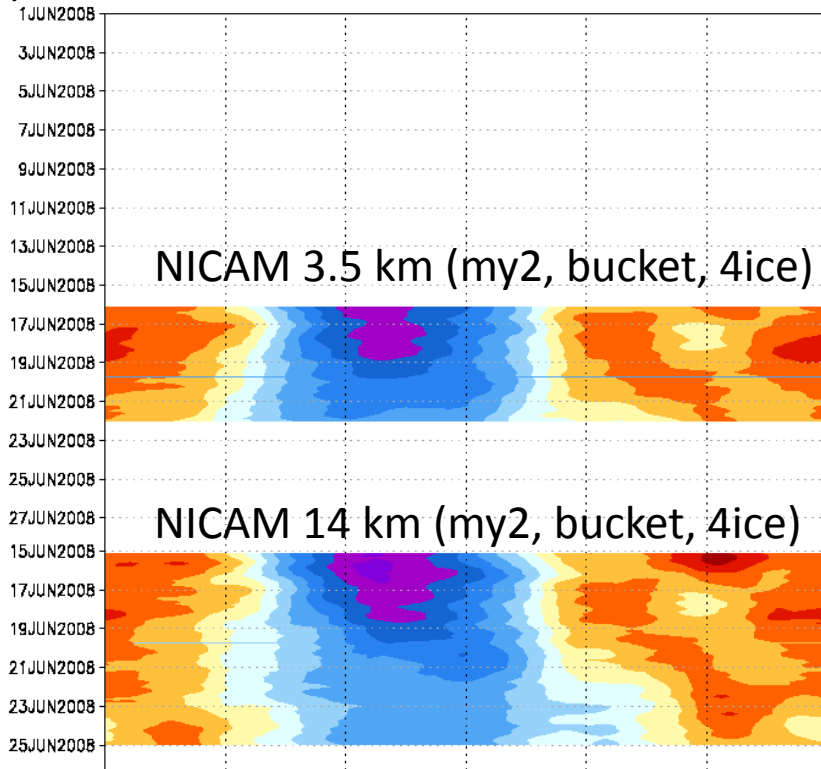
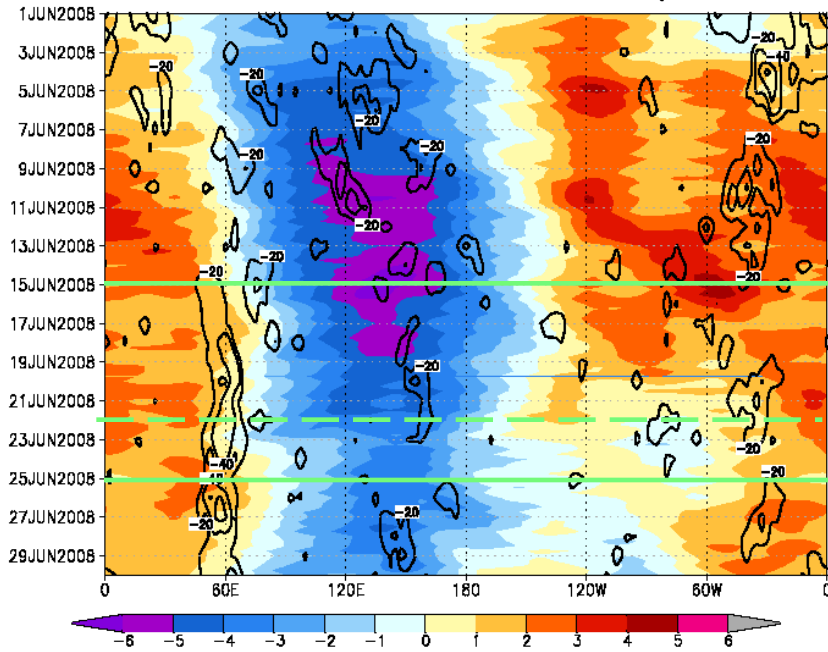
NOAA

OLR (7.5N-7.5S)

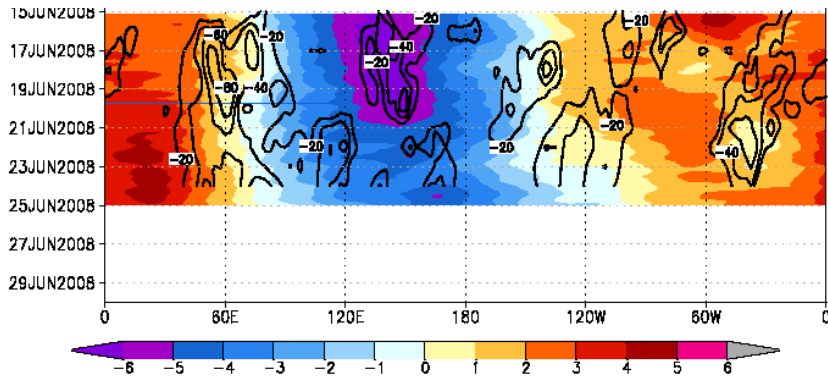


ECMWF YOTC

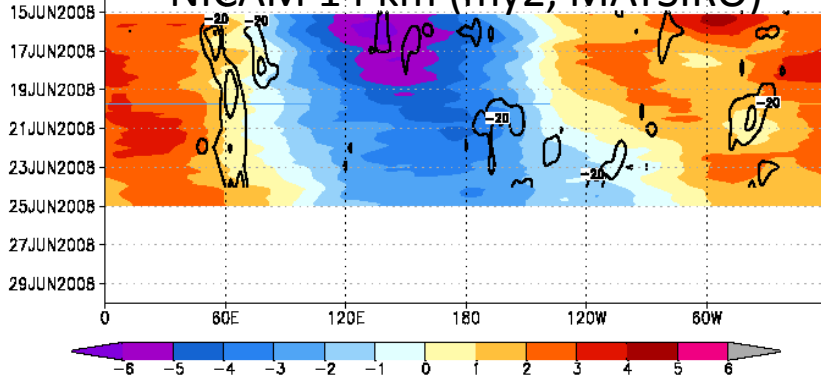
VP200 (7.5N-7.5S)



NICAM 14 km (mynn2.5, MATSIRO)



NICAM 14 km (my2, MATSIRO)



Reproducibility of MJO phase (VP200) in NICAM 2008/06

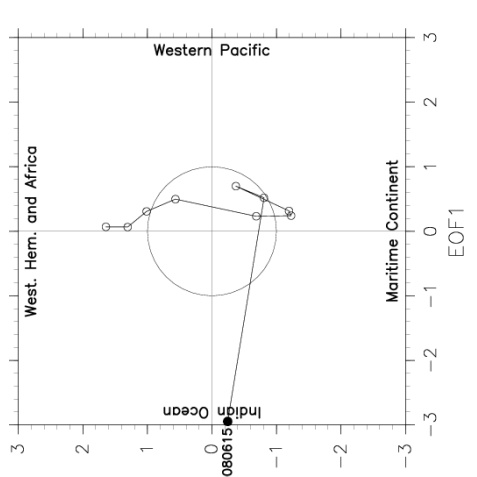
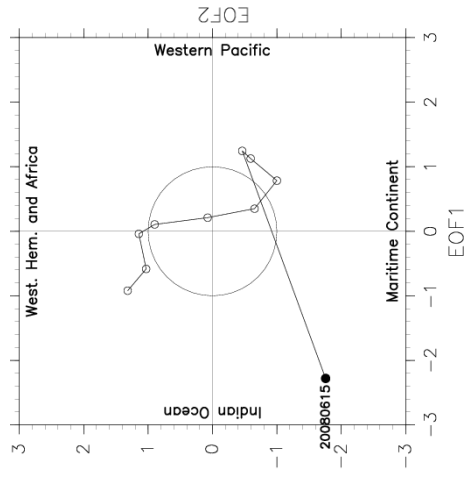
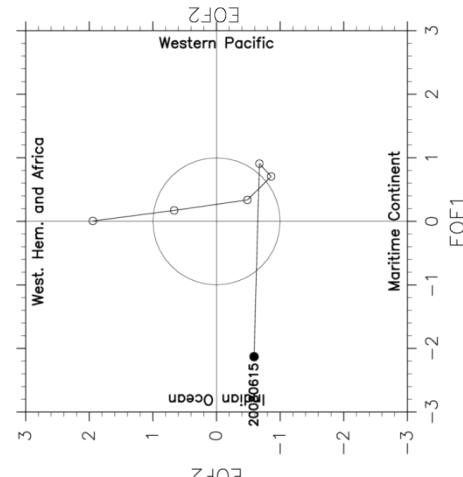
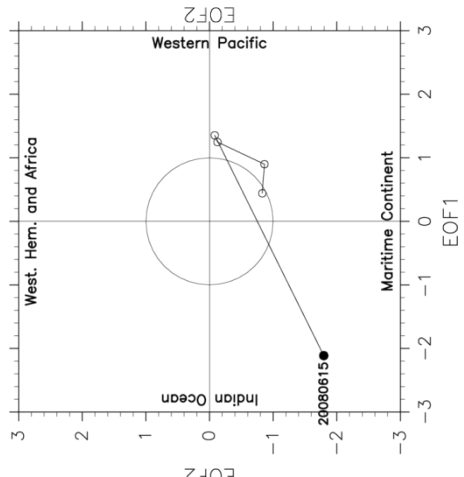
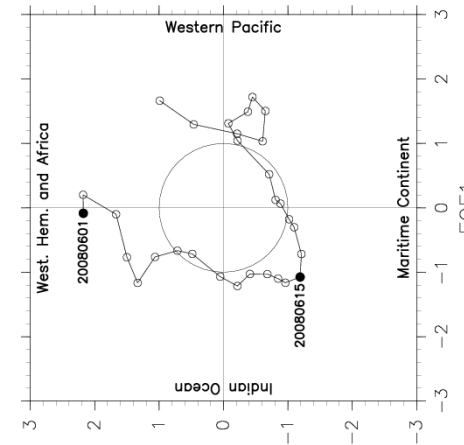
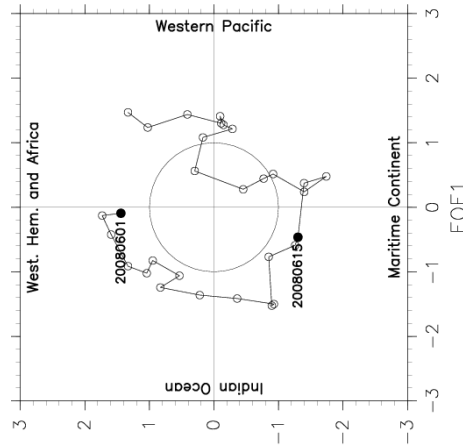
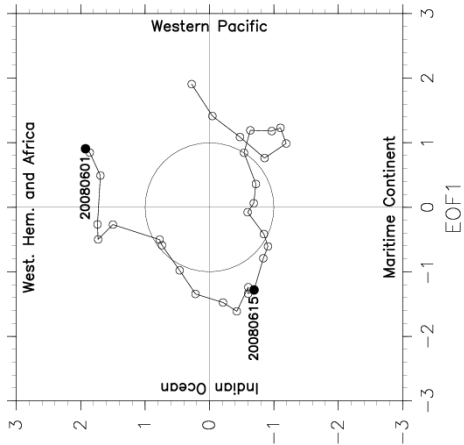
Taniguchi et al. (2010)

Reanalysis

ECMWF YOTC

JCDAS

NCEP



3.5km_MY2

14km_MY2

14km_MY2_MAT

14km_MYNN2.5_MAT

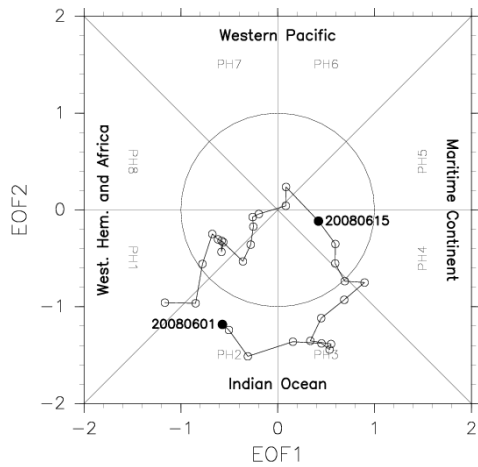
NICAM

Reproducibility of MJO phase (U850,U200, OLR) in NICAM (Jun 2008)

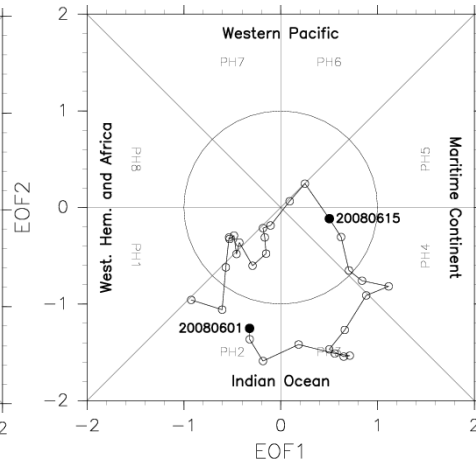
Wheeler and Hendon (2004)

Reanalysis

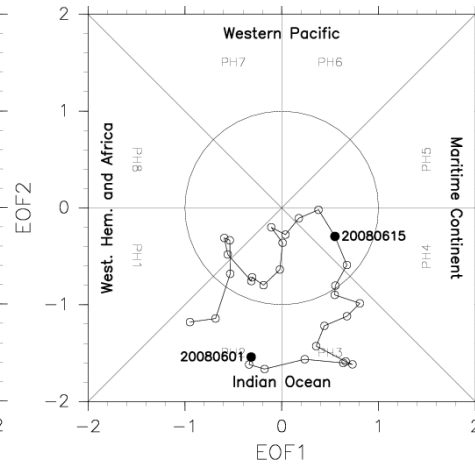
ECMWF YOTC



JCDAS



NCEP



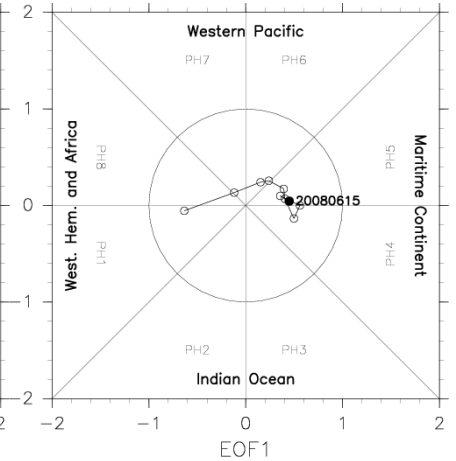
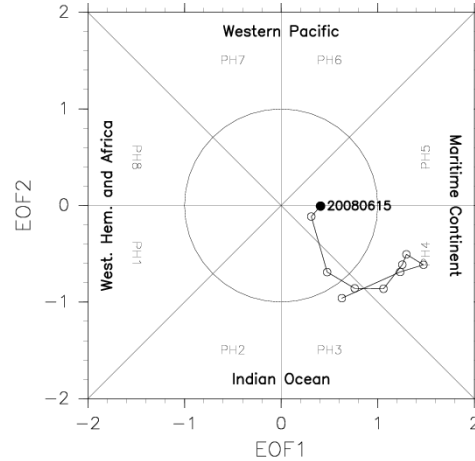
3.5km_MY2

14km_MY2

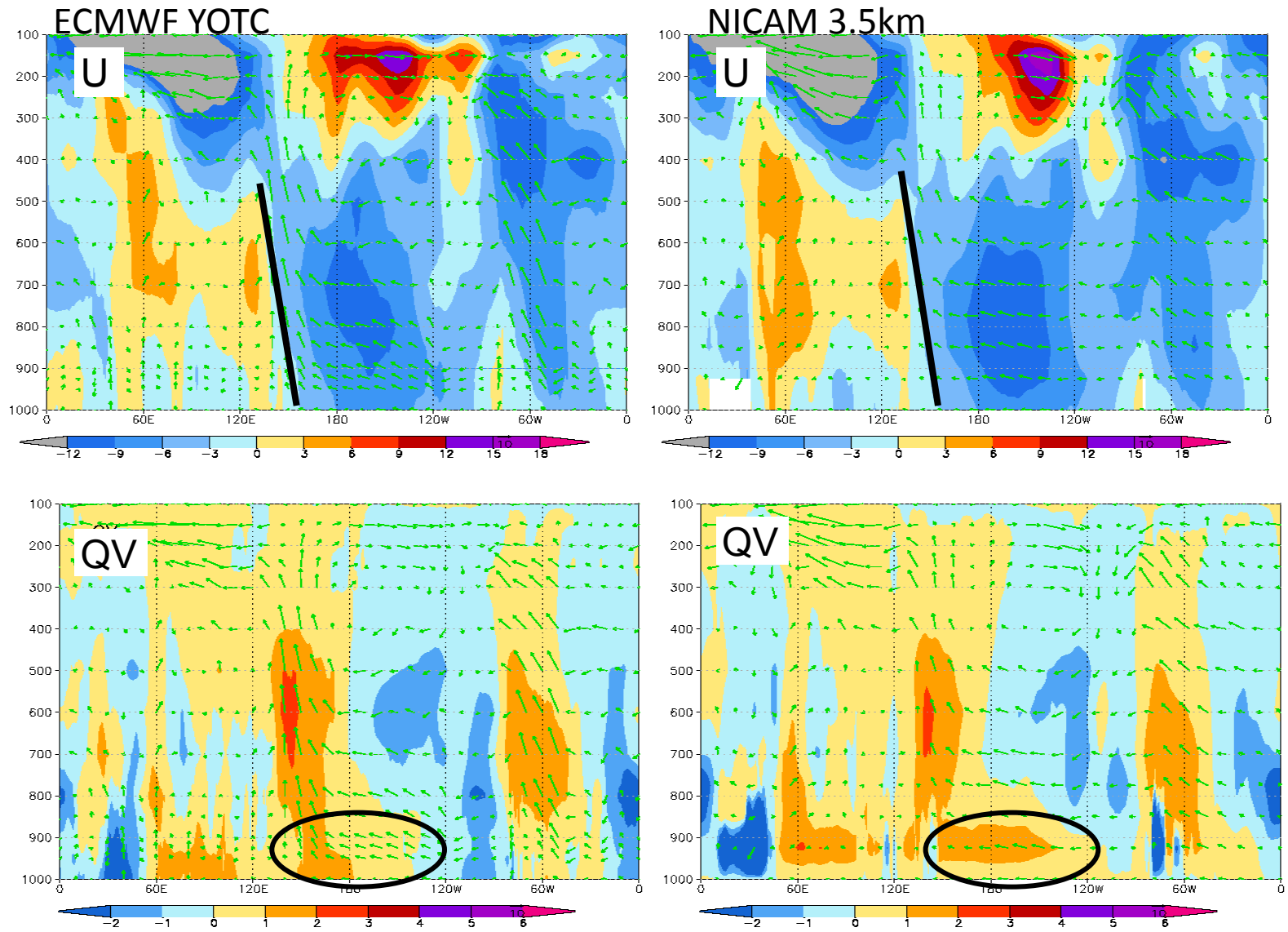
14km_MY2_MAT

14km_MYNN2.5_MAT

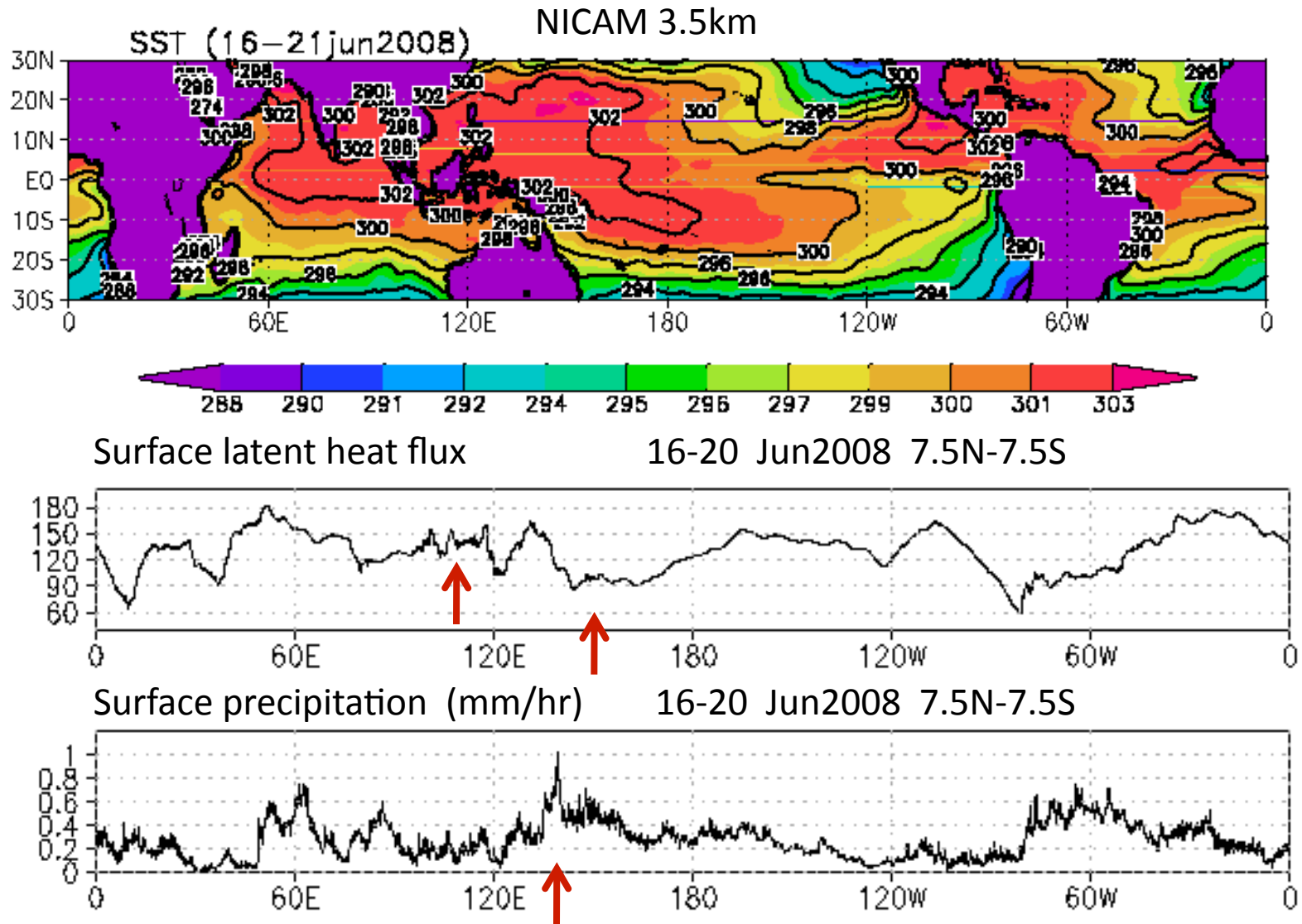
NICAM



Vertical structure (7.5N-7.5S) 16-20 Jun 2008) MJO phase 6-7



Surface flux (7.5N-7.5S) 16-20 Jun 2008 MJO phase 6-7



Consistent with Kim et al. (2009) Fig.9 ?

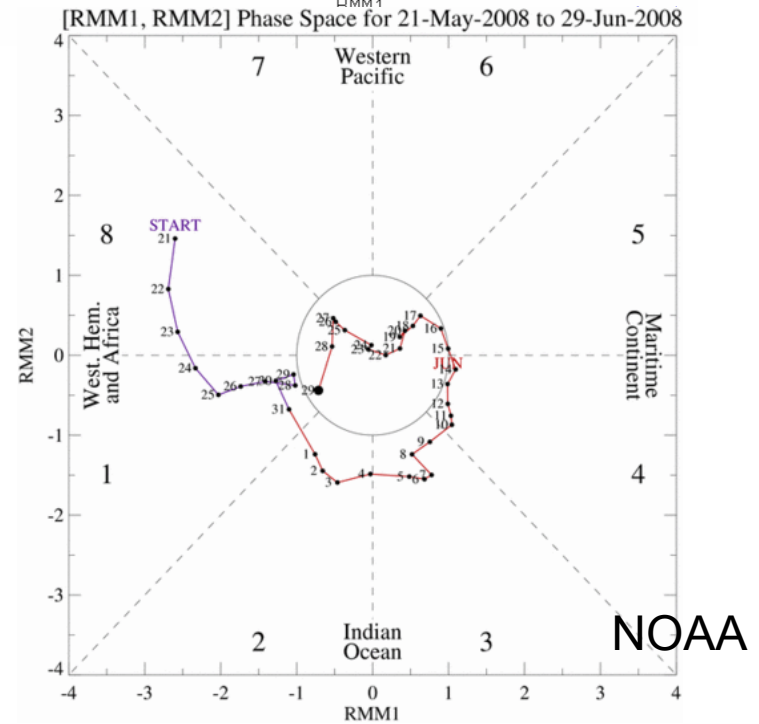
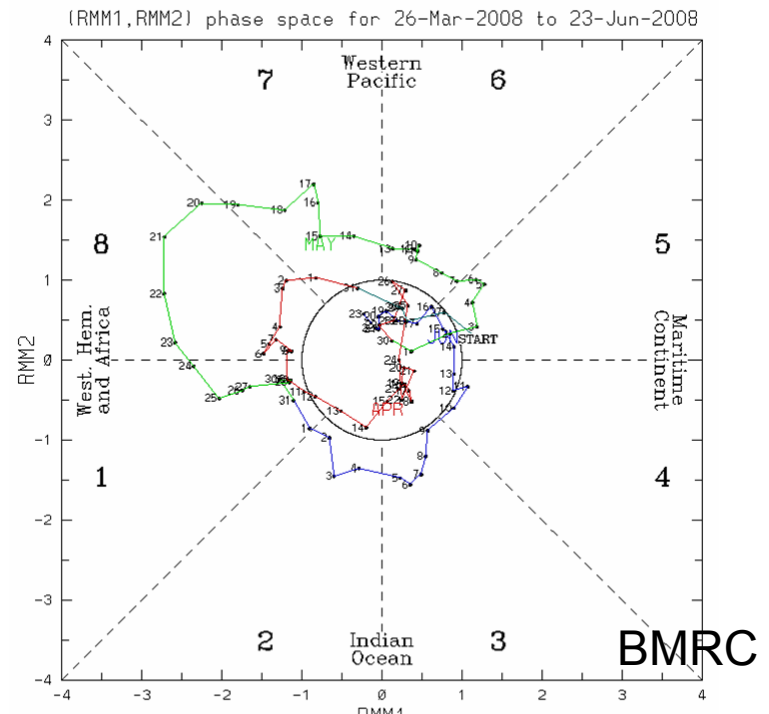
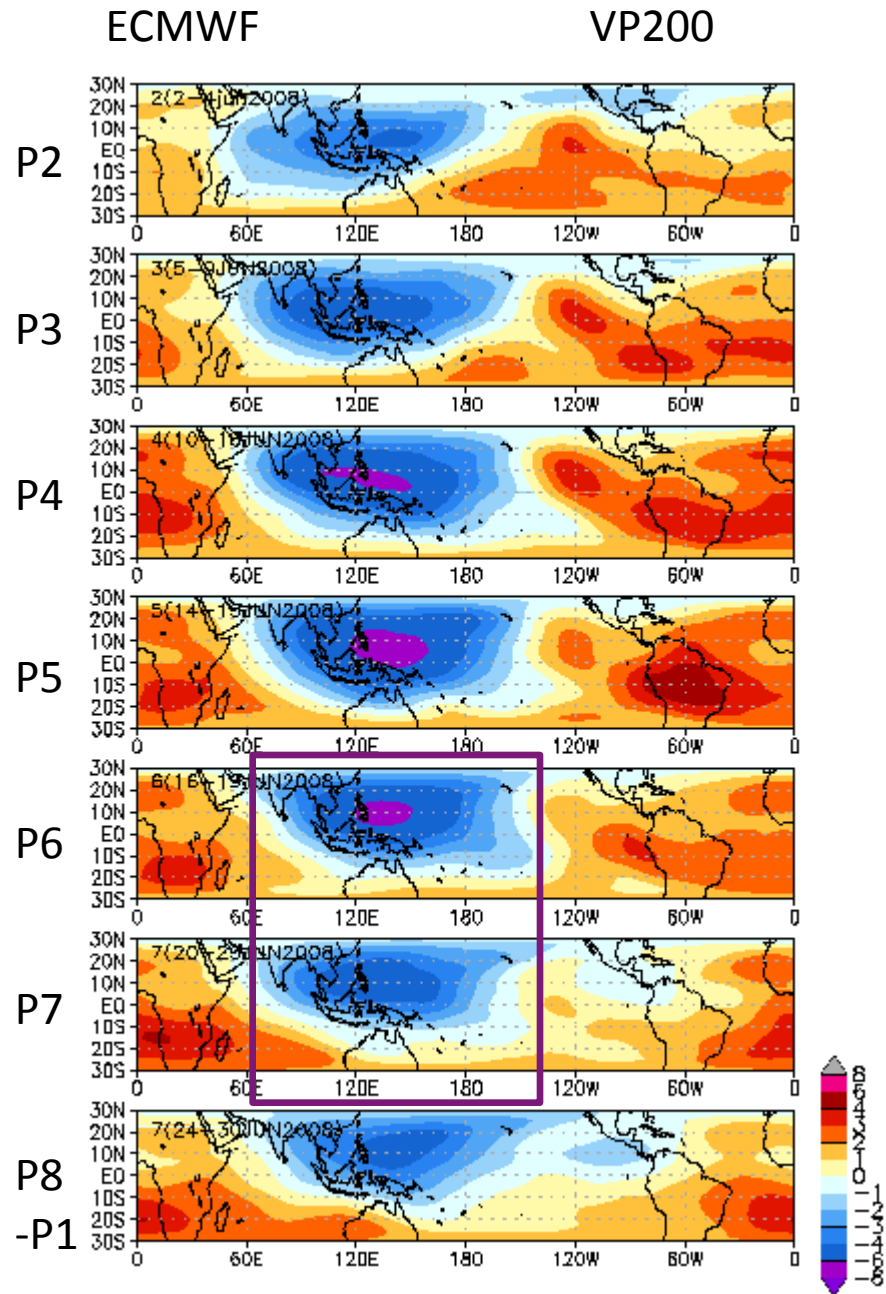
Summary & Future plan

- NICAM simulations suggest potential ability of GCRM in study of multi-scale mechanisms associated with monsoon and ISV (e.g., TC genesis, convectively coupled waves; latent heating, moisture transport, CMT and air-sea interactions in ISV)
- MJO index using VP200 is useful for GCRM simulations (OLR is sensitive to model physics).
- Strategy to better simulate of Monsoon and ISV:
 1. Sensitivity study of model physics (e.g., cloud microphysics, turbulence, slab ocean, land)
 2. Collaboration with field observation projects and validation using satellite data are underway.
- Extension of integration period (~ 1 year) and ensemble simulations (1 \sim 3 month) using 7, 14 km mesh are planned.
 - MJO diagnostics by CLIVAR MJO WG is applicable.

Acknowledgement

- This research was supported by the Core Research for Evolutional Science and Technology program of the Japan Science and Technology Agency, and by the Innovative Program of Climate Change Projection for the 21th century (KAKUSHIN) project "Global Cloud Resolving Model Simulations toward More Accurate and Sophisticated Climate Prediction of Cloud/precipitation Systems" funded by Ministry of Education, Culture, Sports, Science and Technology (MEXT).
- ECMWF YOTC operational data was used to initialize and validate the simulation using NICAM (Jun 2008 case).

appendix

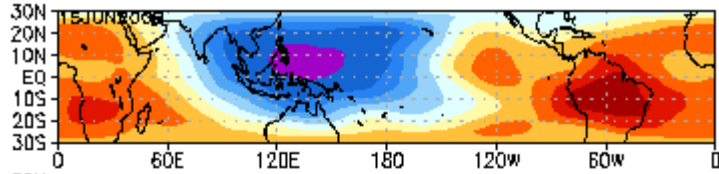


ECMWF

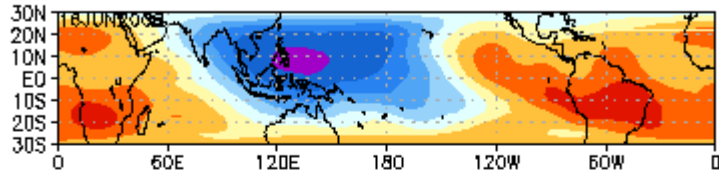
VP200

NICAM 14 km my2 MATSIRO

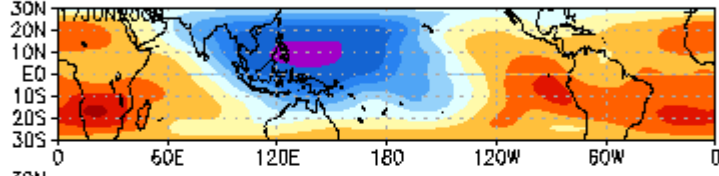
6/15



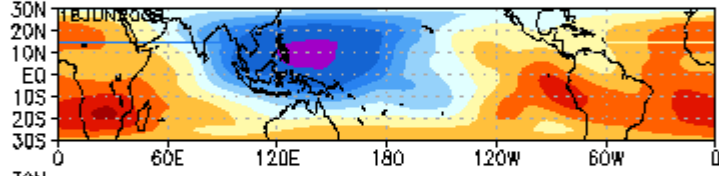
6/16



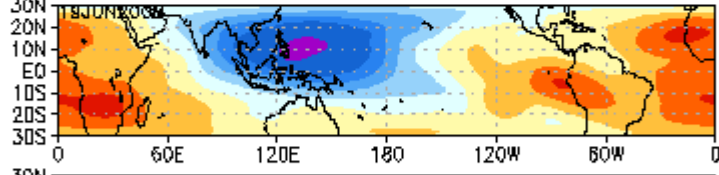
6/17



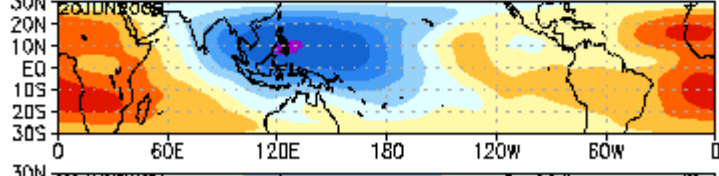
6/18



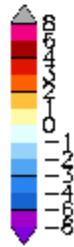
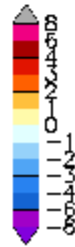
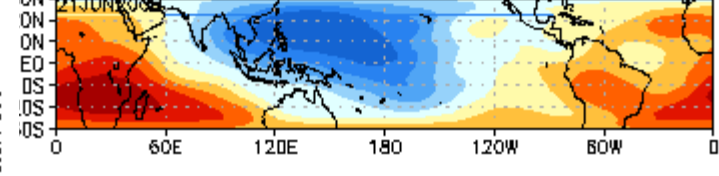
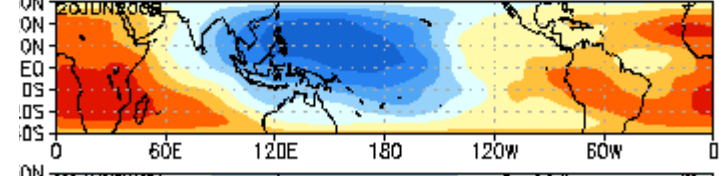
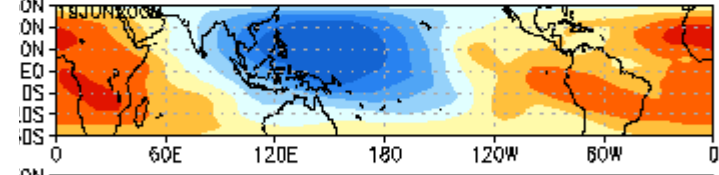
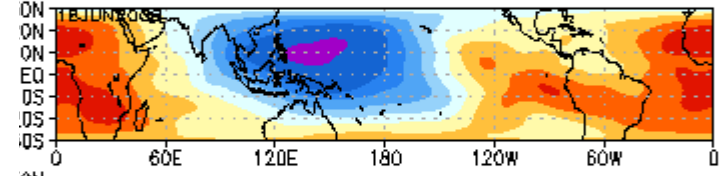
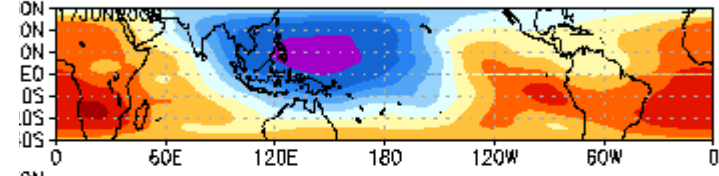
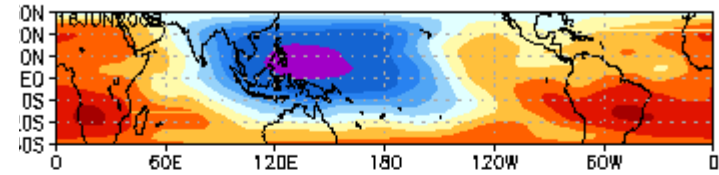
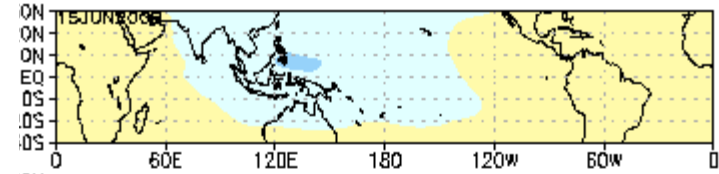
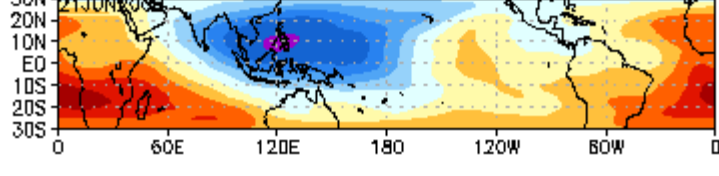
6/19



6/20

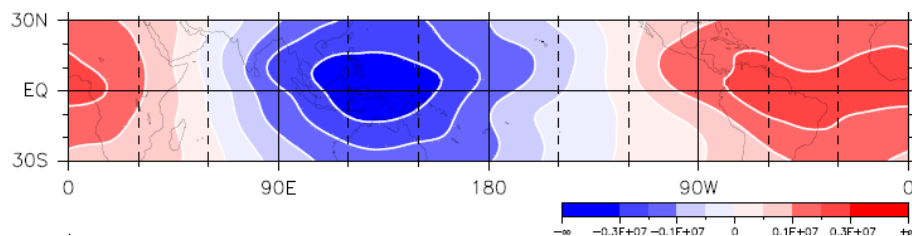


6/21

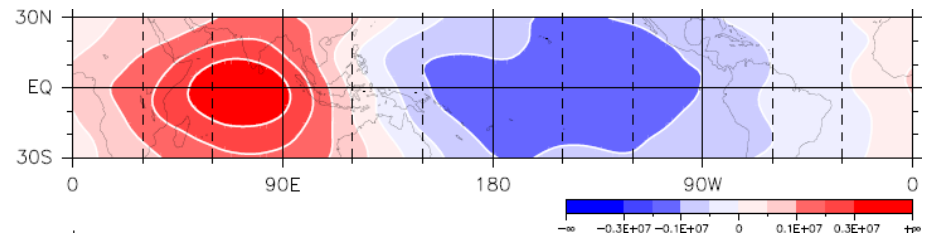


MJO index by CHI200 (Matthews, 2000; Taniguchi et al., 2008)

- It is based on a pair of empirical orthogonal functions of velocity potential anomaly at 200 hPa (**CHI200**) data.
- Methodology
 1. Creating daily data of CHI200 (1xdaily) from intended data
 2. Creating low-pass filtered (60-day) daily climatology data of JRA-25 data from 1979-2007
 3. Preparing anomaly data of intended daily data (1.) from climatology data (2.).
 4. Creating band-pass filtered (30-90 day) anomaly data (3.)
 5. Calculate EOF modes of band-pass filtered data (4.)



JRA-25(1979-2007), EOF1 (40.5%)



JRA-25(1979-2007), EOF2 (34.0%)

Moisture (925hPa) 16-20 Jun 2008 MJO phase 6-7

